이학박사 학위논문

Inhibition of MEK with trametinib enhances the efficacy of anti-PD-L1 monoclonal antibody by regulating anti-tumor immunity in head and neck squamous cell carcinoma

두경부암에서 항 PD-L1 단일 클론 항체의 효능 증진을 위한 MEK 억제제 trametinib 의 항 종양 면역 반응 조절에 관한 연구

2019 년 2 월

서울대학교 대학원

협동과정 종양생물학전공

강 성 호

A Thesis of the Degree of Doctor of Philosophy

두경부암에서 항 PD-L1 단일 클론 항체의 효능 증진을 위한 MEK 억제제 trametinib 의 항 종양 면역 반응 조절에 관한 연구

Inhibition of MEK with trametinib enhances the efficacy of anti-PD-L1 monoclonal antibody by regulating anti-tumor immunity in head and neck squamous cell carcinoma

February 2019

The Department of Cancer biology
Seoul National University
College of Medicine
Seong-Ho Kang

두경부암에서 항 PD-L1 단일 클론 항체의 효능 증진을 위한 MEK 억제제 trametinib 의 항 종양 면역 반응 조절에 관한 연구

지도교수 허 대 석

이 논문을 이학 박사 학위논문으로 제출함

2018 년 10 월

서울대학교 대학원

의학과 협동과정 종양생물학 전공

강 성 호

강성호의 이학박사 학위논문을 인준함

2019 년 1 월

위 원 장 _____(인)
부위원장 _____(인)
위 원 _____(인)
위 원 _____(인)
위 원 _____(인)

Inhibition of MEK with trametinib enhances the efficacy of anti-PD-L1 monoclonal antibody by regulating anti-tumor immunity in head and neck squamous cell carcinoma

by

Seong-Ho Kang

(Directed by Professor Dae Seog Heo, M.D., Ph.D.)

A Thesis Submitted to the Interdisciplinary Graduate Program in partial fulfillment of the requirement of the Degree of Doctor of Philosophy in Cancer Biology at Seoul National University College of Medicine

October 2018

Approved by Thesis Committee:

January 2019

Professor _____ Chairman

Professor _____ Vice chairman

Professor _____

Professor _____

Professor _____

ABSTRACT

강 성 호 (Seong-Ho Kang)
종양생물학과 (Cancer biology)
The Graduate School
Seoul National University

Purpose: Current advances in our understanding of tumor immune escape leads to new field of immunotherapy in cancer treatment, including head and neck squamous cell carcinoma (HNSCC). However, still only a fraction of patients respond to anti-PD-1/PD-L1 monoclonal antibodies (mAbs). In this study, we investigated the effects of MEK inhibitor trametinib on the expression of immune-associated molecules, MHC class I, PD-L1 and T-cell recruiting chemokines, CXCL9 and CXCL10, in human HNSCC cell lines. Then, we assessed the therapeutic efficacy of trametinib combined with an anti-PD-L1 mAb *in vivo*, using SCCVII mouse syngeneic tumor model for HNSCC.

Methods: Six human HNSCC cell lines (SNU-1041, SNU-1066, SNU-1076, Detroit 562, FaDu and HN31) and a mouse squamous cell carcinoma cell line (SCCVII) were used. We conducted MTT cell viability assay using these cell lines after treatment with trametinib for 72 hours. MHC class I and PD-L1 expression levels were analyzed by flow cytometry after treatment with trametinib and/or interferon-gamma (IFN-γ). Expression of PD-L1, Erk1/2, STAT1, STAT2, STAT3, STAT5 and STAT6 were analyzed by Western blotting. STAT1, STAT3 and STAT6 were knocked down by siRNA transfection using lipofectamine. To determine the levels of CXCL9 and CXCL10 transcripts after trametinib treatment, quantitative real-time PCR was carried out. Protein levels of CXCL9 and CXCL10 were determined using

ELISA and intracellular flow cytometry. We evaluated the combinatorial therapeutic effect of MEK inhibitor and an anti-PD-L1 mAb in syngeneic mouse SCCVII squamous cell carcinoma model.

Results: The growth inhibition by trametinib was variable between cell lines with moderate sensitivity (10 nM < IC_{50} < 100 nM in four of six human cells). IC_{50} values were over 10 μM in Detroit 562 and FaDu. Trametinib upregulated MHC class I and PD-L1 expression in human HNSCC cell lines, and this occurred via STAT3 activation. Trametinib also further upregulated the increase in CXCL9 and CXCL10 expression caused by IFN-γ in HNSCC cells, which is associated with T cell infiltration in tumor tissues. Finally, we evaluated the therapeutic efficacy of trametinib combined with an anti-PD-L1 mAb *in vivo*, using SCCVII mouse syngeneic tumor model for HNSCC. While neither PD-L1 blockade nor trametinib treatment alone affected tumor growth, the combined therapy significantly delayed tumor growth. Our results indicate that in the combined therapy trametinib increases $CD8^+$ T cell infiltration in the tumor site and upregulates antigen presentation, and this may be associated with enhanced PD-L1 blockade efficacy.

Conclusions: Our results suggest that immune evasion mechanisms in HNSCC could be counteracted by combination therapy with a MEK inhibitor and anti-PD-1/PD-L1 mAb to inhibit tumor growth.

Keywords: Head and neck squamous cell carcinoma, MEK inhibitor, anti-PD-1/PD-L1 mAb, immune recognition, immune infiltration

***Student number**: 2015-30612*

CONTENTS

LIST OF TABLES AND FIGURES

INTRODUCTION

Cancer immune evasion, which is characterized by disrupted antigen presentation and dysfunction of anti-tumor immune cells, such as cytotoxic T lymphocytes (1, 2), affect the carcinogenesis process, as well as metastasis and the recurrence of head and neck squamous cell carcinoma (HNSCC) (2, 3). To override the suppression of anti-tumor immune response, immune checkpoint inhibitors (ICIs) have been developed to target the PD-1/PD-L1 pathway that have shown remarkable and durable therapeutic efficacy in HNSCC (4, 5). However, only approximately 15-20% of patients respond to this treatment strategy. Therefore, additional therapies are needed that can be used in combination with ICIs to increase their efficacy and response rate (6).

Several anticancer agents have been shown to modulate the immune system via off-target effects, suppressing tumor growth by enhancing anti-tumor immunity in the preclinical stages (7-12). These agents act through multiple mechanisms, which include i) the release of danger signals and inflammatory cytokines by necrotic/apoptotic cells, ii) upregulation of tumor antigen/antigen processing machinery components, iii) depletion or reprogramming of suppressive immune cell subsets, such as tumor-associated macrophage (TAM), myeloid-derived suppressor cell, and regulatory T cells (Tregs) and iv) induction of tumor infiltration by $CD8^+$ T cells. Moreover, the effects of several of these anticancer agents on ICI efficacy are currently being assessed in clinical trials (13-15).

Importantly, of these agents, MAPK pathway inhibitors have been reported to counteract immune evasion mechanisms in the tumor microenvironment, as oncogenic mutations in this pathway are associated with immunosuppression (11, 16-22). Inhibitors of components of the MAPK pathway (such as BRAF and/or MEK) increased the expression of tumor-associated antigen (TAA) and

T cell infiltration, thereby potentiating anti-tumor T cell immune responses. Meanwhile, PD-L1 expression appears to be variably associated with the MAPK pathway, depending on the experimental context; specifically, MAPK pathway inhibitors can up- or down-regulate PD-L1 expression in tumor cells (11, 17, 23). While BRAF inhibitors exert its function only in tumors with BRAF mutations as well as are not effective in *KRAS*-mutated tumors, MEK inhibitors do not require genetic mutations in this pathway and could overcome resistance induced by BRAF inhibitors. Therefore, MEK inhibitors have been evaluated in clinical studies for *RAS*- and/or *RAF*-mutated solid tumors in combination with BRAF inhibitors and these combinations have improved survival of patients (24). Given that studies evaluating immunomodulating activity of MAPK pathway inhibitors also have been done almost in melanoma which have frequent *BRAF* mutations, clinical trials evaluating the efficacy of a MAPK pathway inhibitor in combination with ICIs have been performed mostly on *RAS*/*RAF*-mutated solid cancer patients (13).

Frequently, overexpression of EGFR and activation of its downstream MAPK pathway are observed in HNSCC patients, while they usually lack mutations in MAPK pathway (25, 26). Previous report showed that a MEK inhibitor, selumetinib, upregulates HLA-ABC expression and results in increased T-cell activation as well as IL-2 production by lymphocytes in papillary thyroid cancer cell lines, even in the absence of MAPK mutations (27). Therefore, the aim of this study was to investigate the effects of the MEK inhibitor on immune-related phenotypes of human HNSCC cell lines *in vitro*. Furthermore, we used a syngeneic mouse squamous cell carcinoma model (SCCVII) to evaluate the therapeutic efficacy of combining a MEK inhibitor with an anti-PD-L1 blockade. Of the most clinically studied MEK inhibitors, we chose trametinib which is a highly selective and the first FDA-approved MEK inhibitor for treatment of patients with *BRAF*^{V600E}-mutated metastatic

melanoma and suppresses cell growth more effectively than selumetinib (data not shown).

MATERIALS AND METHODS

1. Cell lines and cell culture

Human HNSCC cell lines SNU-1041, SNU-1066, SNU-1076 cells (purchased from Korean Cell Line Bank, Seoul, Korea) and HN31 cells (obtained from John F. Ensley, Wayne State University) (28) were maintained in RPMI 1640 supplemented with 10% FBS and 10 μg/ml gentamycin. Detroit 562 and FaDu cells (purchased from American Type Culture Collection, Manassas, VA) were maintained in EMEM supplemented with 10% FBS, 100 U/ml penicillin and 100 μg/ml streptomycin. Murine SCC cell line SCCVII cells (29) were maintained in RPMI 1640 supplemented with 10% FBS, 10 mM HEPES, 1 mM sodium pyruvate, 10 μM MEM non-essential amino acids, 2 mM L-glutamine, 55 μM 2-mercaptoethanol, 100 U/ml penicillin and 100 μg/ml streptomycin. Cell lines, except mouse SCCVII cells, were authenticated using PowerPlex 18D System (Promega, Madison, WI) (Table 1). All cells were cultured for less than three months and routinely tested for mycoplasma negative (Fig. 1).

2. Primary T cell isolation from umbilical cord blood mononuclear cells (UCBMC)

Human cord blood naive T cells were positively isolated using MACS CD3 microbeads (Miltenyi Biotech, Bergisch Gladbach, Germany) after Ficoll separation. Purified cells (>95% purity) cells were suspended in RPMI 1640 supplemented with 10% FBS and 10 μg/ml gentamycin.

2. Reagents and antibodies

Trametinib (from Selleckchem, Houston, TX) was dissolved in DMSO for *in vitro* experiments and suspended in a mixture of 0.5% hydroxypropyl methyl

Cell line / Locus	SNU-1041	SNU-1066	SNU-1076	Detroit 562	FaDu	HN31
D5S818	9	9, 11	9, 12	11, 12	12	12, 13
D13S317	8, 12	8, 12	8, 10	12	8, 9	11, 12
D7S820	8, 12	12	11, 12	8, 10	11, 12	10
D16S539	10	9, 11	13	11	11	11, 12
vWA	14, 18	17, 18	16	16	15, 17, 18	15, 18
TH01	7, 9	7, 8	6	8	8	7, 9
TPOX	9, 11	8	8, 11	8, 10	11	6, 11
CSF1PO	10	11	11, 12	11, 13	12	10, 12
AMEL	X	X	X, Y	X		X
D3S1358	15	17	15	14, 15, 16, 17	17, 18	16
D21S11	29	28	30	28, 30	31.2	28
D18S51	15	19	14	15	16	13, 16
D8S1179	12, 13	11, 16	10, 15	13	13	15, 17
FGA	24, 25	23	24, 25	21	25	20, 24
D2S1338	20, 22	17, 26	19, 23.3, 24	25	19	21, 25
D19S433	13, 14	12.2, 14.2	15.2	14	14, 16	13
Penta D	11	12	9, 10	13	11	2.2
Penta E	11, 13	14, 16	12, 22	13	19	8, 12

Table 1. Short tandem repeat (STR) profiling results of human HNSCC cell lines

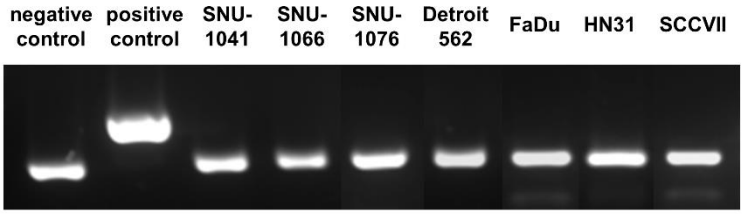

Figure 1. Cell lines are negative for mycoplasma contamination. Cell cultures were screened for mycoplasma contamination using PCR amplification method.

cellulose and 0.2% TWEEN 80 for *in vivo* injections. For *in vivo* experiments, we used a rat anti-mouse PD-L1 monoclonal antibody (mAb) (10F.9G2) and a rat IgG2b isotype control (LTF-2) from BioXCell (West Lebanon, NH). Both the recombinant human (R&D Systems, Minneapolis, MN) and mouse IFN-γ (PeproTech, Rocky Hill, NJ) were reconstituted with 0.1% BSA in PBS and stored at -80℃ before use in experiments. Phorbol myristate acetate (PMA) and ionomycin (Sigma, St. Louis, MO) were resolved in DMSO and stored at -20℃ before use. Primary antibodies against p-STAT1 (Tyr701), STAT1, STAT2, p-STAT3 (Ser727), STAT3, STAT5, p-STAT6, STAT6, p-p44/42 MAPK (Thr202/Tyr204), p44/42 MAPK, CD274 and GAPDH (Cell Signaling Technology, Danvers, MA) were used for Western blotting. Antibodies against mouse CD8 and CD274 (Cell Signaling Technology, Danvers, MA) were used for immunohistochemistry (IHC). Fluorochrome-labeled mAbs for the following markers were used in flow cytometry: anti-human HLA-ABC (G46-2.6), anti-human CD274 (MIH1), anti-mouse CD274 (MIH5), anti-mouse CD25 (PC61), anti-mouse CD8 (53-6.7), anti-mouse CD4 (RM4-5), anti-human CXCL9 (B8-11) and anti-human CXCR3 (1C6/CXCR3) (BD Biosciences, San Jose, CA); anti-mouse CD45 (30-F11), anti-mouse CD3 (eBio500A2), anti-mouse Foxp3 (NRRF-30) and anti-mouse CXCL9 (MIG-2F5.5) (Thermo Fisher Scientific, Waltham, MA); anti-mouse H-2K^{k} (36-7-5), anti-mouse CD11b (M1/70), anti-mouse F4/80 (BM8), anti-mouse CD279 (RMP1-30), anti-mouse Ly-6G (1A8), anti-mouse CXCR3 (CXCR3-173) and anti-human CXCL10 (J034D6) (BioLegend, San Diego, CA). Protein transport inhibitor, GolgiStop (BD Biosciences, San Jose, CA), was used to block CXCL9 and CXCL10 secretion for 12 hours and to block IFN-γ secretion for 5 hours before intracellular flow cytometry staining.

3. Cell viability assay

A total of 2.5 x 10^3 cells (human cell lines) and 1.2 x 10^3 cells (mouse SCCVII cell line) per well were dispensed into 96-well culture plates. After cells had adhered to the plate, they were treated with trametinib for 72 hours. Cell growth inhibition was analyzed using the EZ-Cytox cell viability assay (Dogen, Seoul, Korea) and CellTiter Glo-Luminescent cell viability assay (Promega, Madison, WI). The absorbance was measured with a microplate reader (BioTek, Winooski, VT) at 450 nm for EZ-Cytox cell viability assay. The luminescent signal was measured with a luminescence counter (Perkin Elmer, Waltham, MA) for Cell Titer Glo-Luminescent cell viability assay.

4. Flow cytometry

For surface staining, cells were incubated with fluorochrome-conjugated mAbs for 20 minutes at 4℃. For intracellular Foxp3 staining, Foxp3/Transcription factor staining buffer set (Thermo Fisher Scientific, Waltham, MA), and for intracellular CXCL9, CXCL10 and IFN-γ staining, Fixation/Permeabilization solution kit (BD Biosciences, San Jose, CA) was used according to the manufacturer's instructions. For *ex vivo* experiments, freshly isolated cells were pre-incubated with anti-mouse CD16/CD32 mAb (2.4G2, BD Biosciences, San Jose, CA) to block the binding of antibody to FcγIII/II receptor and then stained with fixable viability dye (Thermo Fisher Scientific, Waltham, MA) prior to antibody staining to exclude dead cells. Data were acquired using FACSCalibur or FACSCanto II (BD Biosciences, San Jose, CA) and analyzed with FlowJo software (Tree Star, Inc., Ashland, OR)

5. Western blotting

Cells were resuspended with cell lysis buffer (Cell Signaling Technology, Danvers, MA) containing protease inhibitor cocktail (Sigma, St. Louis, MO),

PMSF (Sigma, St. Louis, MO) and PhosSTOP (Merck, Kenilworth, NJ) at 4℃ for 20 minutes. After centrifuging at 13,000 rpm at 4℃ for 15 minutes, the supernatant was harvested. Equal amounts of proteins were separated on an SDS-polyacrylamide gel (Thermo Fisher Scientific, Waltham, MA) and transferred to PVDF membrane (Bio-Rad, Hercules, CA), which was then blocked with 5% skim milk at room temperature for one hour, probed with diluted primary antibodies at 4℃ overnight, and with diluted secondary antibodies conjugated to HRP at room temperature for 2 hours. The signals were developed using ECL detection reagent (GE Healthcare, Chicago, Illinois) and visualized with ImageQuant LAS 4000 mini (GE Healthcare, Chicago, Illinois). GAPDH was used as a loading control.

6. siRNA transfection

SNU-1041 cells were transfected with STAT1-, STAT3-, STAT6- or non-targeting siRNAs (Santa Cruz, Dallas, Texas) using Lipofectamine RNAiMAX transfection reagent (Thermo Fisher Scientific, Waltham, MA) according to the manufacturer's instruction. Transfected cells were treated with trametinib for 72 hours followed by flow cytometry and Western blotting.

7. Quantitative real-time RT-PCR (qRT-PCR)

Total RNA from cultured cells and mouse *ex vivo* isolated cells were extracted using RNeasy Mini Kit (Qiagen, Hilden, Germany) and reverse transcribed into cDNA with Superscript III first-strand synthesis system (Thermo Fisher Scientific, Waltham, MA). Quantification of gene expression was conducted using *Power* SYBR green PCR Master Mix and StepOnePlus Real-Time PCR system (Thermo Fisher Scientific, Waltham, MA). GAPDH

was used as an internal reference gene. Primer sequences we used are listed in Table 1.

8. Enzyme-linked immunosorbent assay (ELISA)

Soluble CXCL9 and CXCL10 levels in culture supernatants were measured using DuoSet ELISA (R&D Systems, Minneapolis, MN) according to the manufacturer's instructions.

9. Immunohistochemistry

Formalin-fixed paraffin-embedded tissue sections (4 μm) were deparaffinized, rehydrated and subjected to heat-induced antigen retrieval with Tris-EDTA buffer (for PD-L1 analysis) or citrate buffer (for CD8 analysis). Sections were incubated in 10% normal goat serum at room temperature for one hour, in diluted primary antibodies at 4℃ overnight, in peroxidase blocking solution (0.3% H_2O_2 in PBS) at room temperature for 15 minutes, and finally in diluted secondary antibodies conjugated to HRP at room temperature for 30 minutes. Signals were developed using the DAB chromogen (Dako, Santa Clara, CA) and visualized with a Bright field and Fluorescence Slide Scanner (Leica, Wetzlar, Germany).

10. *In vivo* SCCVII syngeneic model

Mouse SCCVII cells (5×10^5) were injected subcutaneously into the flank of seven-week-old, female, C3H/HeN mice and BALB/c nude mice (Orient Bio Inc., Seongnam, Korea). Tumor volume was measured using a caliper and calculated as: (length x $width^2$)/2. The mice were randomized to four groups and drug treatments began when tumor volume reached 100 ± 25 (mean ± SD) mm^3. Trametinib (1 mg/kg) was administered by oral gavage daily, and anti-PD-L1 mAb (10 mg/kg) was intraperitoneal injected twice per weekly. Mice

Gene			Primer sequence (5’ → 3’)
Human	*CXCL9*	Forward	GGAGATCACCAGTGTGTGGCT
		Reverse	AGGCACTGCATTGTGGTAGGA
	CXCL10	Forward	AATCGATGCAGTGCTTCCAAGG
		Reverse	GCAGCTGATTTGGTGACCATCATT
	GAPDH	Forward	TGACCCCTTCATTGACCTC
		Reverse	TTCCCGTTCTCAGCCTTG
Mouse	*H-2Kk*	Forward	ACTGGAGCTGTGGTGGCTTT
		Reverse	CACCAAGTCCACTCCAGGCA
	B2M	Forward	GCTCGGTGACCCTGGTCTTT
		Reverse	CGTAGCAGTTCAGTATGTTCGGCTT
	CXCL9	Forward	TCTGGCTTCCAGAGCCACAC
		Reverse	TCTAGCTCACCAGCAAACAGACA
	CXCL10	Forward	GAGGGCCATAGGGAAGCTTGA
		Reverse	GTGTGTGCGTGGCTTCACTC
	CD274	Forward	TGGCAGGAGAGGAGGACCTT
		Reverse	TGTAGTCCGCACCACCGTAG
	GAPDH	Forward	GGAAAGCTGTGGCGTGATGG
		Reverse	AGCTCTGGGATGACCTTGCC

Table 2. Primer sequences used in qRT-PCR analysis

were euthanized when tumor size exceeded 1,000 mm^3. Tumors, draining lymph nodes (dLNs) and spleens were collected on day 5 for pharmacodynamic analysis. The Institutional Animal Care and Use Committee of Seoul National University Hospital approved all animal studies (approval number: #16-0166-S1A1, #17-0117-S1A0 and #18-0062-S1A0).

11. Statistical analysis

Data are represented as the mean ± SD and were analyzed by GraphPad Prism (GraphPad Software, La Jolla, CA). An unpaired two-tailed student's *t* test was used to determine differences between groups. All *P* values less than 0.05 were considered statistically significant.

RESULTS

The MEK inhibitor trametinib increases MHC class I and PD-L1 expression in human HNSCC cell lines with moderate cellular cytotoxicity

We first tested the susceptibility of six human HNSCC cell lines to the MEK inhibitor trametinib (Fig. 2A). These cell lines do not harbor activating mutations in *RAS* or *RAF* with the exception of HN31, which harbor an *HRAS* G12D mutation (30). Several gene mutation profiles of each cell line we used were shown in Table 3. Growth inhibition by trametinib treatment occurred variably in these cell lines with moderate sensitivity (range of IC_{50}: 10 nM ~ 100 nM, in four of six cells). Based on this, we selected a sub-lethal concentration of trametinib (50 nM), which was used to investigate immunologic changes without lethal damage. As shown in Fig. 2B, trametinib treatment increased MHC class I expression in all cell lines. In addition, trametinib further enhanced exogenous IFN-γ-induced MHC class I upregulation. We also observed that trametinib slightly increased basal and IFN-γ-induced PD-L1 expression in all cell lines, except in SNU-1066, in which trametinib treatment diminished IFN-γ-induced PD-L1 upregulation (Fig. 2C and D).

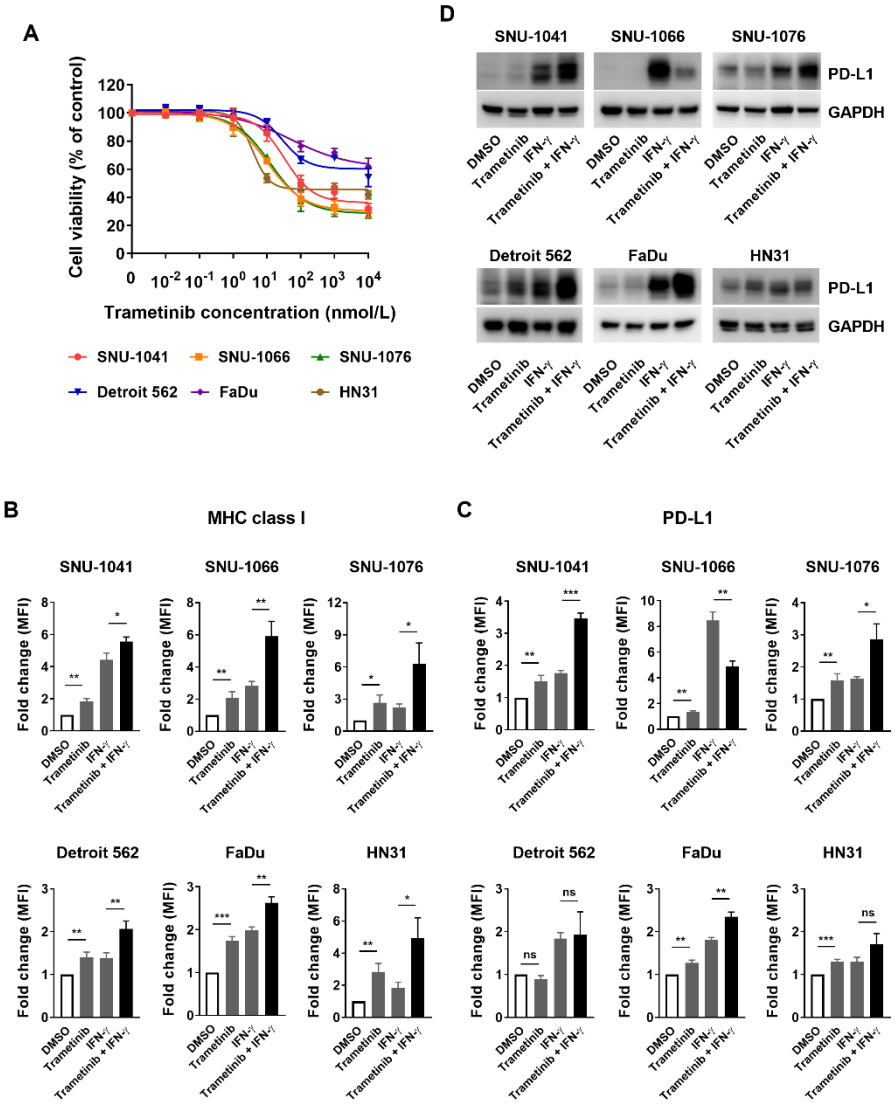
A
Cell viability (% of control)
120
100
80
60
40
20
0
0 10-2 10-1 100 101 102 103 104
Trametinib concentration (nmol/L)
SNU-1041
SNU-1066
SNU-1076
Detroit 562
FaDu
HN31
D
SNU-1041
SNU-1066
SNU-1076
PD-L1
GAPDH
DMSO
Trametinib
IFN-γ
Trametinib + IFN-γ
Detroit 562
FaDu
HN31
B
MHC class I
C
PD-L1
Fold change (MFI)

Figure 2. Trametinib exerts moderate cytotoxic effect on human HNSCC cell lines and increases MHC class I and PD-L1 expression in surviving cells. A, Cells were incubated with 10 pM - 10 µM of trametinib for 72 hours and cell growth inhibition was analyzed using a cell viability assay. Data are shown as the mean ± SD from three independent experiments. **B, C,** Cells were treated with trametinib (50 nM), IFN-γ (1 ng/ml; 10 ng/ml to examine PD-L1 expression in SNU-1066 cells) or the combination of trametinib and IFN-γ (pretreated with DMSO or trametinib one hour prior to the addition of IFN-γ) for 72 hours. Expression of MHC class I **(B)** and PD-L1 **(C)** were assessed by flow cytometry. The fold change in mean fluorescence intensity (MFI) was averaged from three independent experiments. Error bars indicate SD. **D,** Changes in PD-L1 expression shown in Fig. 2C were confirmed by Western blotting. Data show one of three independent experiments with comparable results.

Cell line	Gene	Protein change	Type
SNU-1041	*TP53*	p.G245D	Substitution_missense
	BRCA2	p.G2063E	Substitution_missense
SNU-1066	*TP53*	p.G187_splice	Deletion_Frameshift
	CDKN2A	p.D92fs*54	Deletion_Frameshift
	STAT1	p.K209R	Substitution_missense
	JAK1	p,L50V	Substitution_missense
	TGFBR2	p.S409F	Substitution_missense
	APC	p.E601D	Substitution_missense
	IDH2	p.Q64H	Substitution_missense
SNU-1076	*TP53*	p.KSVT120fs	Deletion_Frameshift
	CDKN2A	p.P114H	Substitution_missense
	PIK3CA	p.H1047R	Substitution_missense
	TLR4	p.E287V	Substitution_missense
Detroit 562	*TP53*	p.R175H	Substitution_missense
		p.R43H	Substitution_missense
		p.R82H	Substitution_missense
	PIK3CA	p.H1047R	Substitution_missense
FaDu	*TP53*	p.R248L	Substitution_missense
		p.V225_splice	Splice_Site_SNP
	BRCA2	p.Q861_fs	Insertion_frameshift
	ERBB3	p.D297H	Substitution_missense
	TGFA	p.A37T	Substitution_missense
	RAF1	p.P614L	Substitution_missense
	ROS1	p.Y2114C	Substitution_missense
HN31	*TP53*	p.C176F	Substitution_missense
	HRAS	p.G12D	Substitution_missense
	CDKN2A	p.M54fs*61	Deletion_frameshift

Table 3. Several mutational characteristics in oncogenes and tumor suppressor genes (TSGs) of human HNSCC cell lines. Oncogenes and TSGs mutated in human HNSCC cell lines were represented from CCLE and COSMIC databsets.

Upregulation of MHC class I and PD-L1 by trametinib is STAT3-dependent

Next, we investigated the effects of trametinib on STAT signaling pathway, as it is known to regulate MHC class I and/or PD-L1 expression (31-34). First, we confirmed that trametinib suppresses Erk1/2 phosphorylation at a concentration of 50 nM we used (Fig. 3A). When we assessed change in STAT phosphorylation upon trametinib and IFN-γ treatment, except for STAT4, whose expression is restricted to myeloid cells, thymus and testes, we found that treatment with trametinib increased p-STAT1 expression, and this effect was enhanced in the presence of exogenous IFN-γ (Fig. 3B). While total STAT1 expression was low, expression was increased after IFN-γ treatment, via input from a positive feedback loop, and this was further enhanced by trametinib in some cells. Furthermore, trametinib treatment activated STAT3 and STAT6 was shown to be activated by trametinib treatment in three of six cell lines. Phosphorylated STAT2 and STAT5 were not detected in any condition of any cell line we used (data not shown).

To determine which signaling molecule was responsible for the upregulation of MHC class I and PD-L1 by trametinib, we knocked down STAT1, STAT3 and STAT6 expression with siRNA transfections. For these experiments, we used SNU-1041 cells, as the change in MHC class I and PD-L1 expression was most prominent in these cells (Fig. 2B-D). After confirming that each STAT expression was efficiently and specifically downregulated at the protein level (Fig. 4A), we found that, interestingly, STAT3 knock-down, but not STAT1 or STAT6, abolished trametinib-induced MHC class I and PD-L1 upregulation (Fig. 4B). We observed that STATs were not involved in these effects in the remaining three siRNA-transfectable cell lines (data not shown).

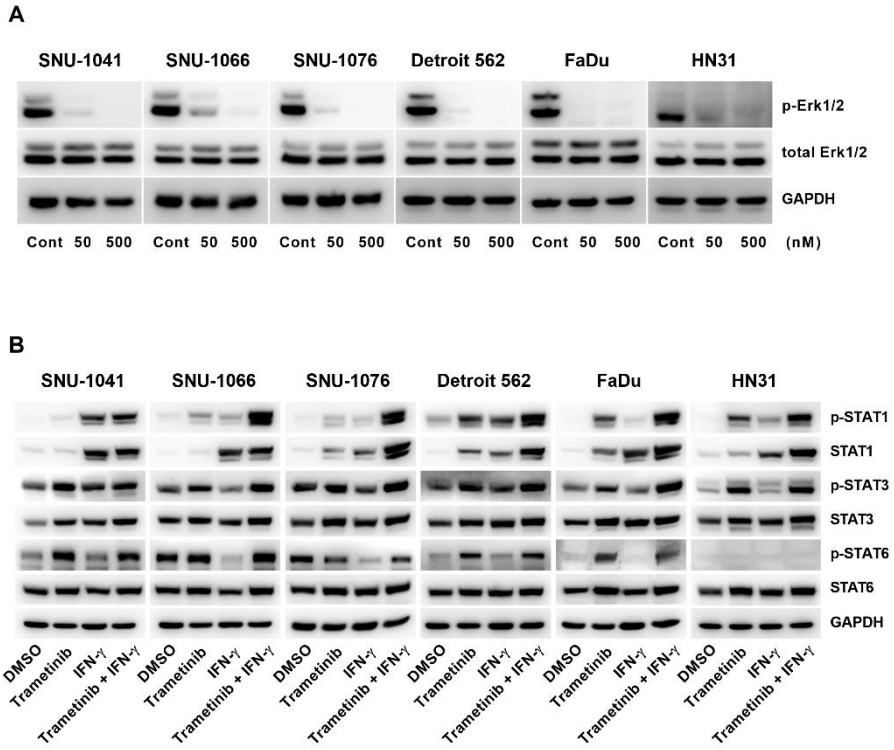

Figure 3. Trametinib increases STAT1, STAT3 and STAT6 phosphorylation while inhibiting Erk1/2 pathway in human HNSCC cell lines. A, Human HNSCC cell lines were treated with the indicated doses of trametinib. After 24 hours, expression of phospho- and total-Erk1/2 were assessed by Western blotting. Representative images from two independent experiments are shown. **B**, Cells were treated with trametinib (50 nM), IFN-γ (1 ng/ml) or the combination of trametinib and IFN-γ (pretreated with DMSO or trametinib one hour prior to the addition of IFN-γ) for 72 hours. Levels of p-STAT1, p-STAT3 and p-STAT6 were examined by Western blotting. Data are representative of three independent experiments.

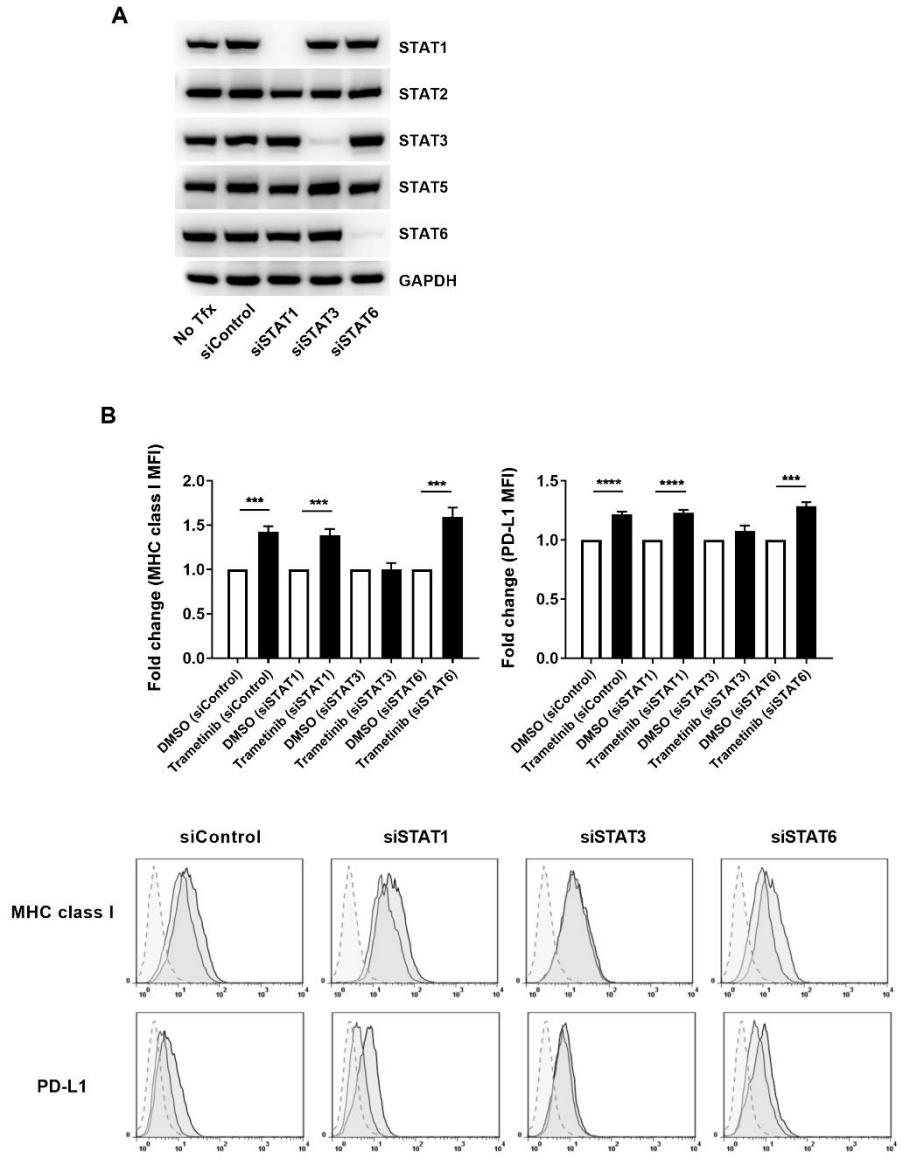
A
STAT1
STAT2
STAT3
STAT5
STAT6
GAPDH
No Tfx
siControl
siSTAT1
siSTAT3
siSTAT6
B
Fold change (MHC class I MFI)
2.0
1.5
1.0
0.5
0.0
***
***
***
DMSO (siControl)
Trametinib (siControl)
DMSO (siSTAT1)
Trametinib (siSTAT1)
DMSO (siSTAT3)
Trametinib (siSTAT3)
DMSO (siSTAT6)
Trametinib (siSTAT6)
Fold change (PD-L1 MFI)
1.5
1.0
0.5
0.0
****
****
***
DMSO (siControl)
Trametinib (siControl)
DMSO (siSTAT1)
Trametinib (siSTAT1)
DMSO (siSTAT3)
Trametinib (siSTAT3)
DMSO (siSTAT6)
Trametinib (siSTAT6)
siControl
siSTAT1
siSTAT3
siSTAT6
MHC class I
PD-L1

Figure 4. STAT3 depletion abolishes the effect of trametinib on MHC class I and PD-L1 expression in SNU-1041 cells. A, SNU-1041 cells were transfected with siControl, siSTAT1, siSTAT3 or siSTAT6. Expression of all STAT family members, except STAT4, was examined by Western blotting in untransfected (No Tfx), siControl, siSTAT1, siSTAT3 or siSTAT6 transfectants, respectively. Representative Western blot from three independent experiments were shown. **B,** SNU-1041 cells were transfected as in (A). MHC class I and PD-L1 expression were analyzed in siRNA-transfected cells after trametinib treatment for 72 hours using flow cytometry. *top*; bar graphs showing the fold change in MFI from three independent experiments (error bars indicate SD), *bottom*; representative histogram showing unstained (dashed line), DMSO (gray) and trametinib (black) treatment.

T cell-recruiting chemokines CXCL9 and CXCL10 are upregulated by trametinib, which synergizes with IFN-γ in human HNSCC cell lines

Increased antigen presentation through MHC class I molecules can be recognized by $CD8^+$ T cells when they are present within the tumor microenvironment. Therefore, we next examined trametinib's effects on levels of the T cell chemoattractants CXCL9 and CXCL10, which are also induced by IFN-γ, in human HNSCC cell lines. As we expected, trametinib treatment significantly induced CXCL9 and CXCL10 mRNA expression (Fig. 5A and B) as well as protein expression (Fig. 5C, D and Fig. 6). Moreover, chemokine expression was even further increased by combined exposure to both trametinib and exogenous IFN-γ. These *in vitro* findings suggest that trametinib treatment facilitates anti-tumor immunity by increasing T cell infiltration and antigen presentation in the tumor; however, PD-L1 blockade is also required, as trametinib induces PD-L1 expression, which may be also upregulated by T cell-derived IFN-γ.

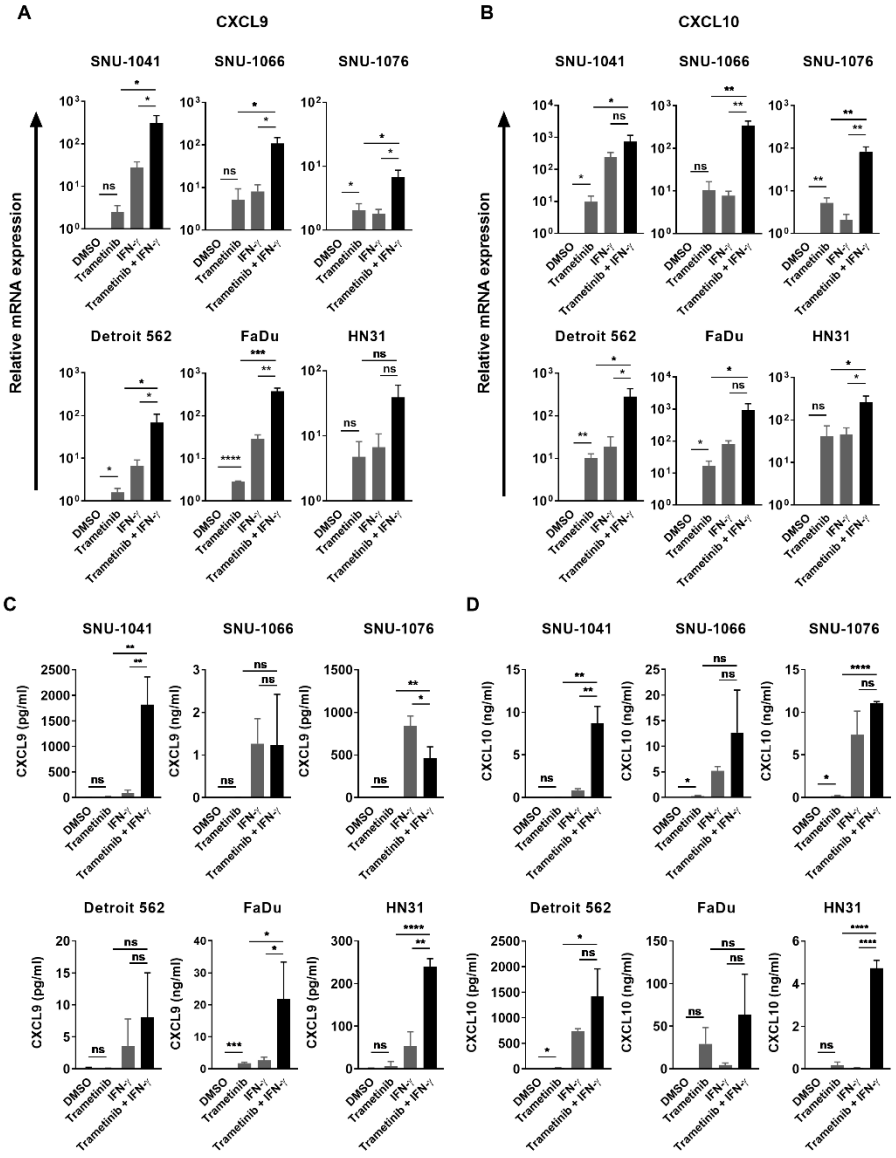
A
CXCL9
SNU-1041
SNU-1066
SNU-1076
Detroit 562
FaDu
HN31
Relative mRNA expression
DMSO
Trametinib
IFN-γ
Trametinib + IFN-γ
B
CXCL10
C
CXCL9 (pg/ml)
CXCL9 (ng/ml)
D
CXCL10 (ng/ml)
CXCL10 (pg/ml)

Figure 5. Trametinib enhances T cell chemoattractants level and synergizes with IFN-γ in human HNSCC cell lines. Cells were treated with trametinib (50 nM), IFN-γ (5 ng/ml) or the combination of trametinib and IFN-γ (pretreated with DMSO or trametinib one hour prior to the addition of IFN-γ) for 72 hours. Expression of CXCL9 **(A)** and CXCL10 **(B)** were determined by qRT-PCR. Results represent gene expression changes in log10 scale ± SD of three independent experiments. Protein levels of CXCL9 **(C)** and CXCL10 **(D)** were measured in culture supernatants by ELISA. Data represents mean ± SD from three independent experiments.

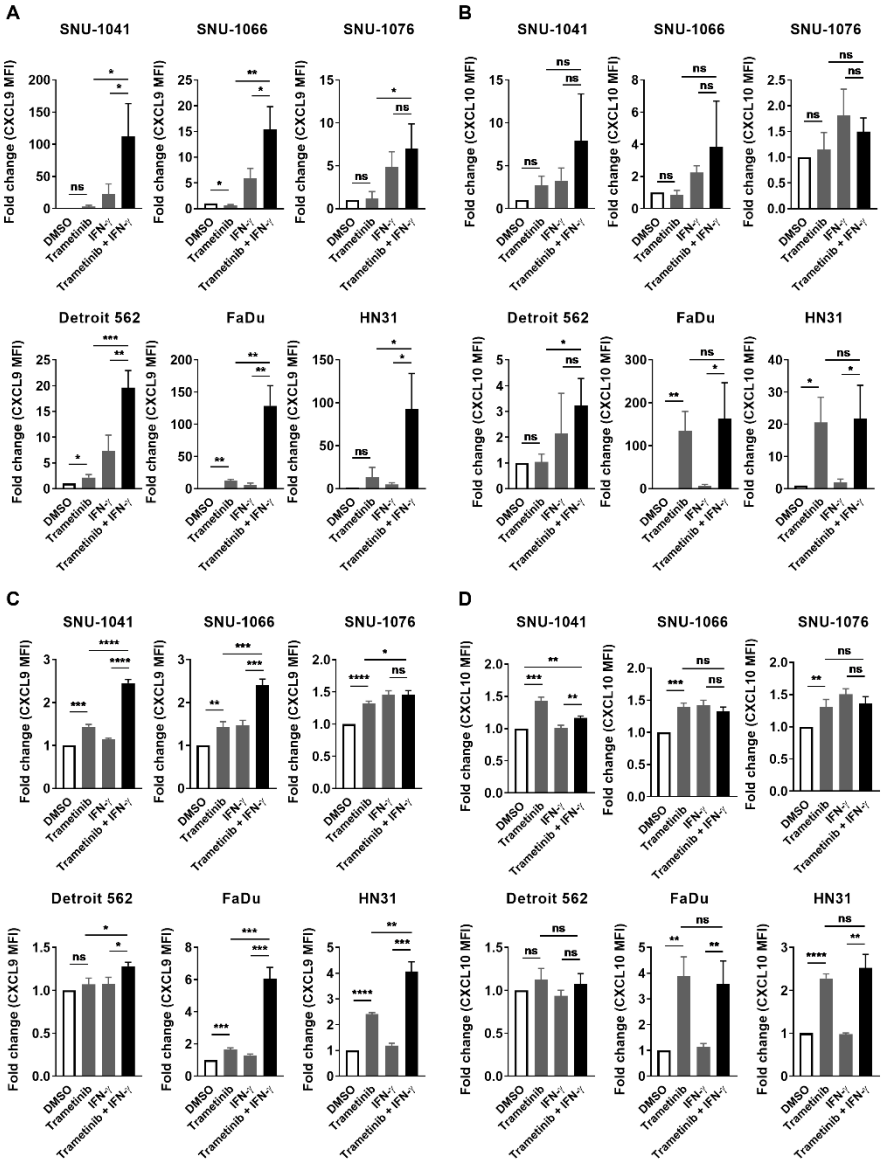
A
SNU-1041
SNU-1066
SNU-1076
Detroit 562
FaDu
HN31
Fold change (CXCL9 MFI)
B
Fold change (CXCL10 MFI)
C
D
DMSO
Trametinib
IFN-γ
Trametinib + IFN-γ
ns

Figure 6. Trametinib upregulates CXCL9 and CXCL10 protein expression and synergizes with IFN-γ in human HNSCC cell lines. Cells were treated with trametinib (50 nM), IFN-γ (5 ng/ml) or the combination of trametinib and IFN-γ (pretreated with DMSO or trametinib one hour prior to the addition of IFN-γ) for 72 hours. Expression of CXCL9 and CXCL10 were assessed by intracellular flow cytometry after treatment with GolgiStop for the last 12 hours of 72 hours. **A, B,** The fold change in percentage of cells expressing CXCL9 **(A)** and CXCL10 **(B)** was averaged from three independent experiments. **C, D,** The fold change in MFI level for CXCL9 **(C)** and CXCL10 **(D)** was averaged from three independent experiments. Error bars indicate SD.

Trametinib exhibited similar effects in an SCCVII mouse cell line

Prior to investigating the therapeutic efficacy of combining trametinib with an anti-PD-L1 mAb in an SCCVII mouse squamous cell carcinoma model, we validated our human HNSCC cell lines observations in SCCVII mouse cells. Trametinib treatment moderately inhibited cell growth with an IC_{50} value of 10 ± 1.2 nM (Fig. 7A). In addition, we found that expression of the MHC-encoded class I molecule H-$2K^k$ was highly induced in live cells in the presence of trametinib, whereas expression of PD-L1 was not changed (Fig. 7B). However, trametinib synergistically induced both PD-L1 and H-$2K^k$ expression in the presence of exogenous IFN-γ.

Interestingly, expression of CXCL9 and CXCL10 was elevated by trametinib with or without IFN-γ (Fig. 7C and D). Erk1/2 activation was suppressed at the concentration of trametinib we used (Fig. 7E). Therefore, we concluded that the SCCVII tumor model was an appropriate model to test our hypothesis, as we found that trametinib increased the antigenicity and immunogenicity of tumor cells by upregulating MHC class I, CXCL9 and CXCL10. However, the concurrent induction of PD-L1 indicated that co-treatment of trametinib with an anti-PD-L1 mAb would be necessary.

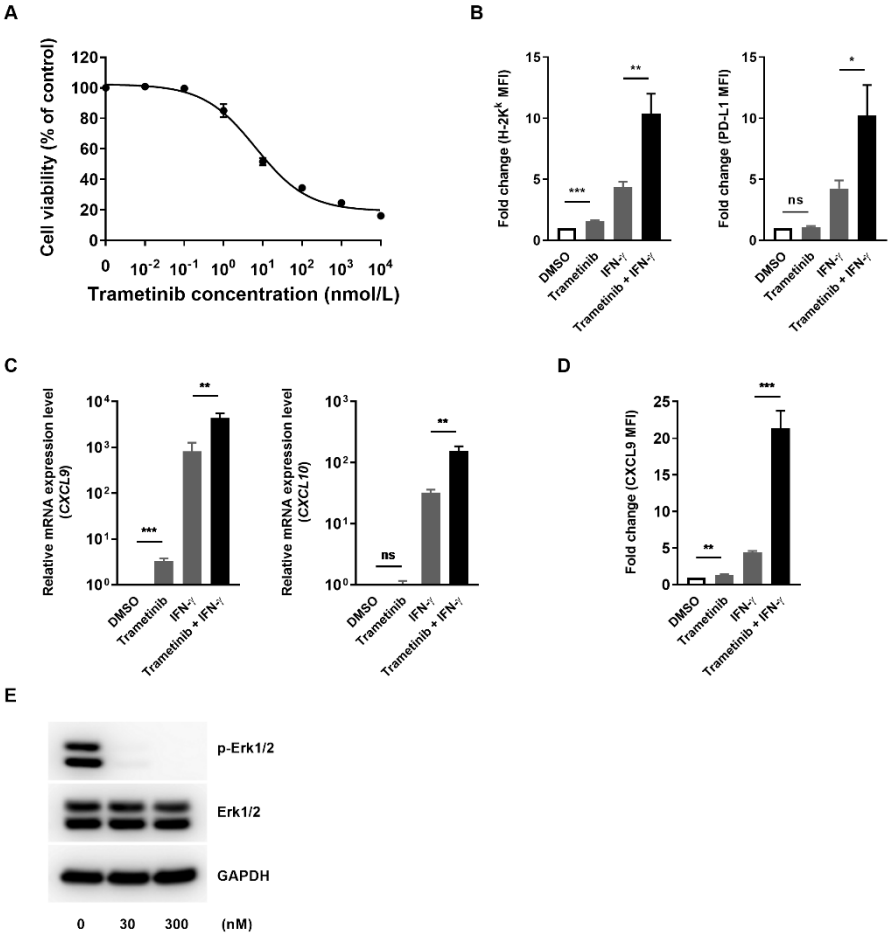
A
Cell viability (% of control)
Trametinib concentration (nmol/L)
B
Fold change (H-2K^k MFI)
Fold change (PD-L1 MFI)
DMSO
Trametinib
IFN-γ
Trametinib + IFN-γ
C
Relative mRNA expression level (CXCL9)
Relative mRNA expression level (CXCL10)
D
Fold change (CXCL9 MFI)
E
p-Erk1/2
Erk1/2
GAPDH
0
30
300
(nM)

Figure 7. *In vitro* evaluation of the immunomodulating activity of trametinib in an SCCVII mouse cell line. A, SCCVII cells were incubated with 10 pM – 10 µM of trametinib for 72 hours and cell growth inhibition was determined using a cell viability assay. Data are the mean ± SD from three independent experiments. **B-D,** SCCVII cells were treated with trametinib (30 nM), IFN-γ (1 ng/ml, **B**; 5 ng/ml, **C and D**) or the combination of trametinib and IFN-γ (pretreated with DMSO or trametinib one hour prior to the addition of IFN-γ) for 72 hours. **B,** The expression of H-2K^k (left) and PD-L1 (right) was assessed by flow cytometry. The fold change in MFI was averaged from three independent experiments. Error bars indicate SD. **C,** Changes in CXCL9 and CXCL10 gene expression were determined by qRT-PCR. Data show the mean ± SD from three independent experiments in log10 scale. **D,** CXCL9 protein levels were analyzed by intracellular flow cytometry after treatment with GolgiStop for the last 12 hours of 72 hours. The fold change in percentage of cells expressing CXCL9 was averaged from three independent experiments. Error bars indicate SD. **E,** Cells were treated with the indicated doses of trametinib. After two hours, the expression of phospho- and total-Erk1/2 was assessed by Western blotting. Data show one of three independent experiments with comparable results.

Combined therapy with trametinib and an anti-PD-L1 mAb delays mouse tumor growth and increases the number of $CD8^+$ tumor-infiltrating T cells

To investigate the *in vivo* efficacy of a combined therapy, compared to each treatment alone, SCCVII cells were implanted subcutaneously in the flank of C3H syngeneic mice. We found that the trametinib dose used was sufficient to inhibit Erk1/2 activation in tumor tissues (Fig. 8A). However, as shown in Fig. 8B, trametinib treatment alone did not delay tumor growth, and anti-PD-L1 mAb monotherapy was also ineffective. In contrast, concurrent combination treatment with trametinib and an anti-PD-L1 mAb resulted in a delay of tumor growth.

Analysis of immune subsets within the tumor microenvironment on the fifth day after treatment revealed an increase in infiltrating $CD8^+$ T cells in trametinib-treated mice (Fig. 9A and B). $CD3^+CD4^+CD25^+Foxp3^+$ Treg cells were slightly decreased by trametinib treatment, but this was not statistically significant. TAMs ($CD11b^+F4/80^+$) were not affected by any treatments. The number of neutrophils ($CD11b^+Ly6G^+$) was decreased by exposure to an anti-PD-L1 mAb, both with or without trametinib. Increased $CD3^+CD8^+$ tumor infiltrating lymphocytes (TILs) were found in mice that received the combined trametinib and an anti-PD-L1 mAb treatment, and this was correlated with longer survival, while there were no significant alterations in other immune subsets (Fig. 10).

The T cell activation marker CD25 was elevated in $CD8^+$ T cells by trametinib treatment (Fig. 11A), and this was also associated with the longer survival observed in mice who received the combination therapy (Fig. 11B). Other activation markers, PD-1, CD69 and T-bet, showed no significant difference between groups (Fig. 11A). To assess the ability of $CD8^+$ T cells to produce IFN-γ, $CD8^+$ T cells isolated from tumor tissue and spleen (and draining lymph nodes (dLNs) at the endpoint analysis), respectively, were

stimulated with PMA and ionomycin *ex vivo*. At early phase, trametinib alone or when combined with an anti-PD-L1 mAb slightly inhibited the production of IFN-γ from $CD8^+$ T cells (Fig. 12A). However, we observed that IFN-γ production was increased by trametinib treatment and it was further enhanced by combination with an anti-PD-L1 mAb at the endpoint (Fig. 12B). Interestingly, treatment with an anti-PD-L1 mAb resulted in a decrease in the total T cells, an increase in $CD25^+$– and $PD\text{-}1^+$– T cells, and an increased proportion of Treg cells in CD4 T cells in the secondary lymphoid organs, whereas trametinib-induced immunological changes were limited to tumor sites (Fig. 13). This indicates that treatment with an anti-PD-L1 mAb regulated systemic immunity. We did not observe any adverse effects associated with immune activation from any of the treatments.

Finally, we confirmed our *in vitro* findings *in vivo*, five days after treatment. Consistent with the *in vitro* data, the mRNA expression of $H\text{-}2K^k$, as well as its associated molecule β2m, were increased by trametinib treatment (Fig. 14A). CXCL9 and CXCL10 transcripts tended to be increased by trametinib and/or anti-PD-L1 mAb treatment, despite variations among mice. As expected, expression of CXCR3, which is a receptor for CXCL9 and CXCL10, increased in splenic T cells after treatment with an anti-PD-L1 mAb, which activate systemic immunity as observed in Fig. 13, because CXCR3 expression is highly increased in activated T cells (Fig. 15A and B) (35). Meanwhile, trametinib was not shown to be involved in increasing CXCR3 expression, but at least to have no negative effects either alone or in combination with an anti-PD-L1 mAb. In more detail, we analyzed CXCR3 expression in naive T cell subset derived from umbilical cord blood mononuclear cells (UCBMCs), since adult peripheral T cells are mixed with different subsets of T cells depending on their activation status. As shown in Fig. 16, the expression of CXCR3 was increased by trametinib treatment in naive T cells including both $CD4^+$ and $CD8^+$ T cells. An

increase in PD-L1 expression in trametinib-treated mice was also observed (Fig. 14A, B and Fig. 17A). The specificity of PD-L1 IHC was investigated using spleens from naïve and tumor-bearing mice (Fig. 17B). When we performed the same experiment as in Fig. 8B using T cell-deficient BALB/c nude mice, there was no tumor growth retardation by the combination of trametinib and an anti-PD-L1 mAb, demonstrating it was attributed to T cells consistent with the above results (Fig. 18). These data indicate that trametinib-induced immunological changes enhance $CD8^+$ T cell responses; however, blockade of the PD-L1 pathway is required for effective control of the tumor growth.

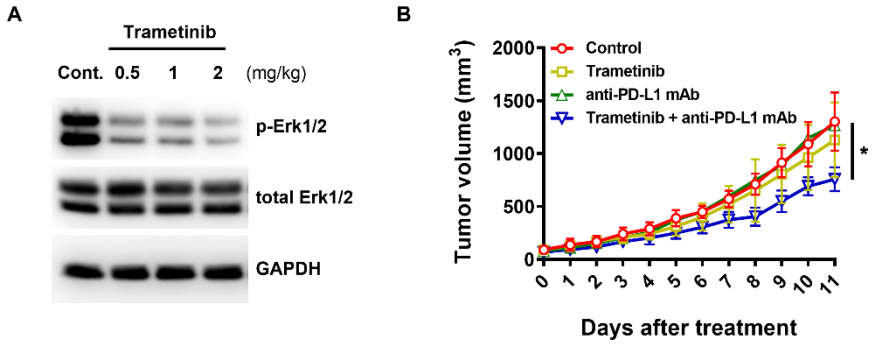

Figure 8. Anti-tumor activity of combined treatment with trametinib and an anti-PD-L1 mAb in an SCCVII syngeneic mouse tumor model. A, Tumor-bearing C3H mice (n=3) received trametinib by oral gavage once daily at the indicated doses. Inhibition of Erk1/2 activation was determined by Western blotting at the endpoint. **B,** Tumor-bearing C3H mice (n=5-6) were treated with trametinib (1 mg/kg) by oral gavage once daily and/or anti-PD-L1 mAb (10 mg/kg) by intraperitoneal (i.p.) injection twice weekly. Control mice received vehicle or isotype control.

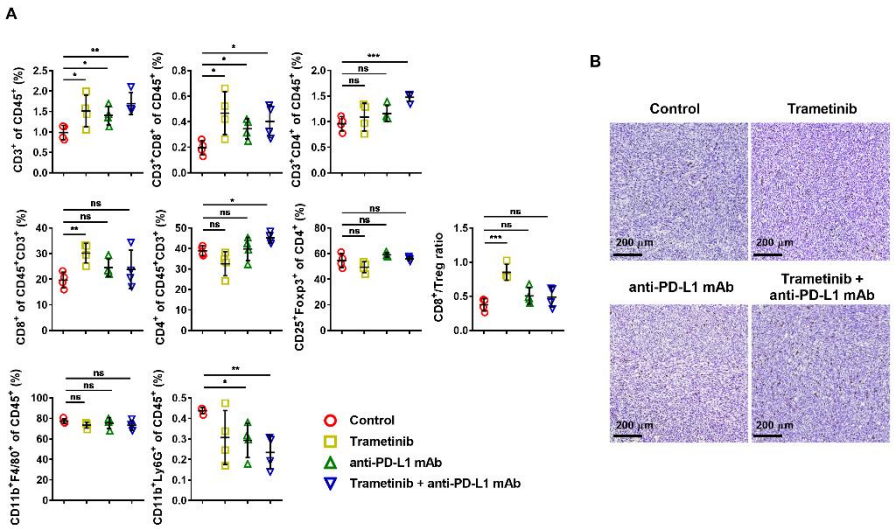

Figure 9. Trametinib treatment with or without an anti-PD-L1 mAb increases CD8$^+$ T cell infiltration in the tumor site after five days of treatment. A, Immune subsets constituting tumor tissue were analyzed using flow cytometry (n=4). Cells were subjected first to gating to eliminate debris, doublets and dead cells, and further analyzed by gating CD45$^+$ cells. **B,** CD8$^+$ T cells within tumor tissues were assessed by IHC staining (n=3). Scale bar indicates 200 μm. Representative data are shown.

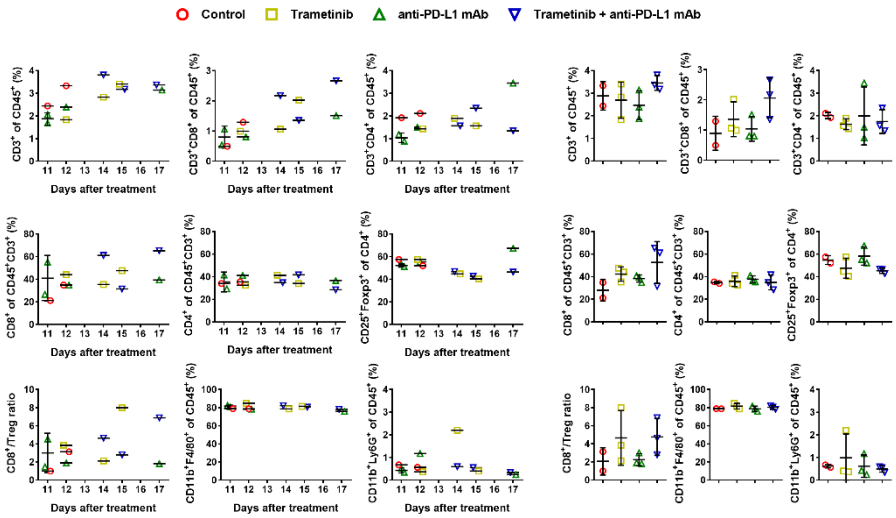

Figure 10. Treatment with trametinib and an anti-PD-L1 mAb specifically increases CD8$^+$ T cells, which is associated with delayed tumor growth. Immune cell subsets were analyzed using flow cytometry after gating CD45$^+$ cells at the endpoints (n=2-4). Graphs represent each immune cell subset from individual mice over time (left) and patterns of each group (right).

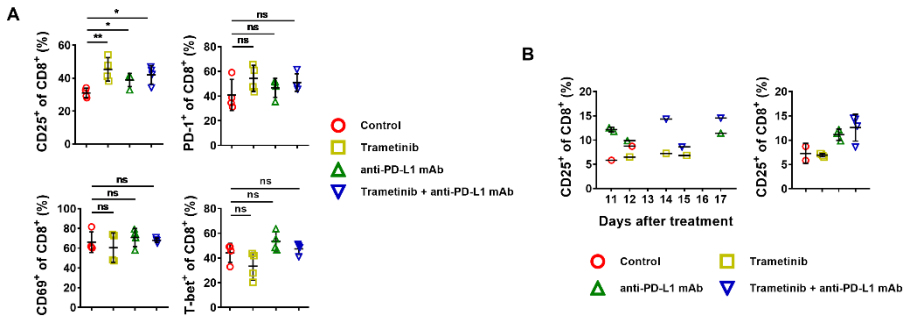

Figure 11. Expression of CD25 is increased by trametinib treatment with or without an anti-PD-L1 mAb and associated with delayed tumor growth by combination treatment. A, B, Levels of the activation markers including CD25 were measured in tumor-infiltrating $CD8^+$ T cells using flow cytometry after five days of treatment (n=4) **(A)** and only CD25 at the endpoint (n=2-4) **(B)**. **B,** Graphs represent CD25 expression from individual mice over time (left) and patterns of each group (right).

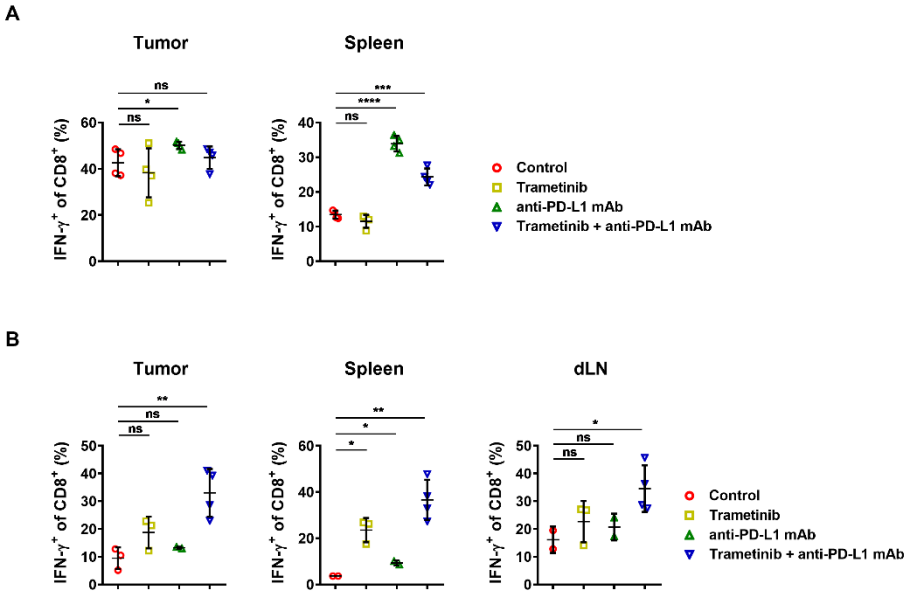

Figure 12. Trametinib enhances the ability of CD8$^+$ T cells to produce IFN-γ at later stage of tumor progression. Cells isolated from each tissue after five days of treatment (n=4) **(A)** and at the endpoint (n=2-4) **(B)** were stimulated with PMA (10 ng/ml) and ionomycin (1 μg/ml) *ex vivo* for 6 hours. To block the secretion of IFN-γ, GolgiStop was treated after one hour of treatment with stimuli. IFN-γ production from CD8$^+$ T cells was measured using flow cytometry.

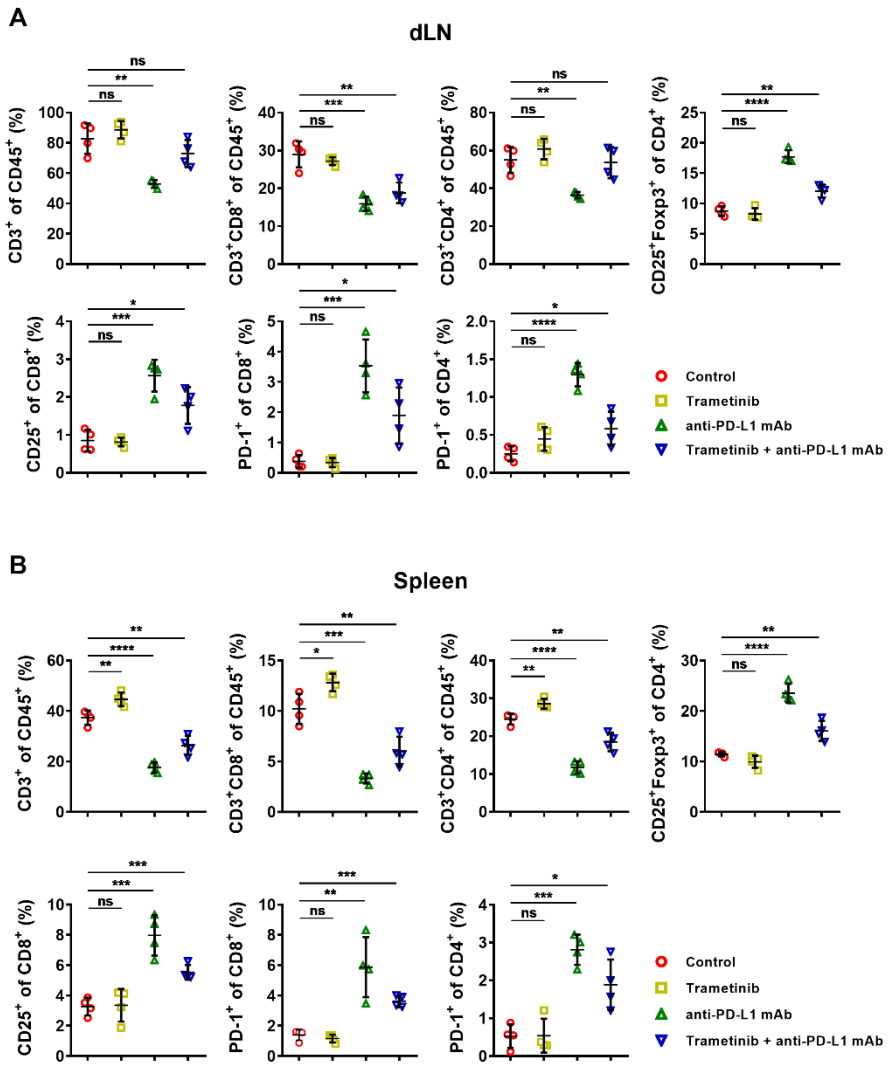

Figure 13. The effects of trametinib on T cells were confined to the tumor tissue, whereas the anti-PD-L1 mAb acted systemically. T cell composition and expression of their activation markers within the tumor-draining lymph node **(A)** and spleen **(B)** were measured using flow cytometry after five days of treatment.

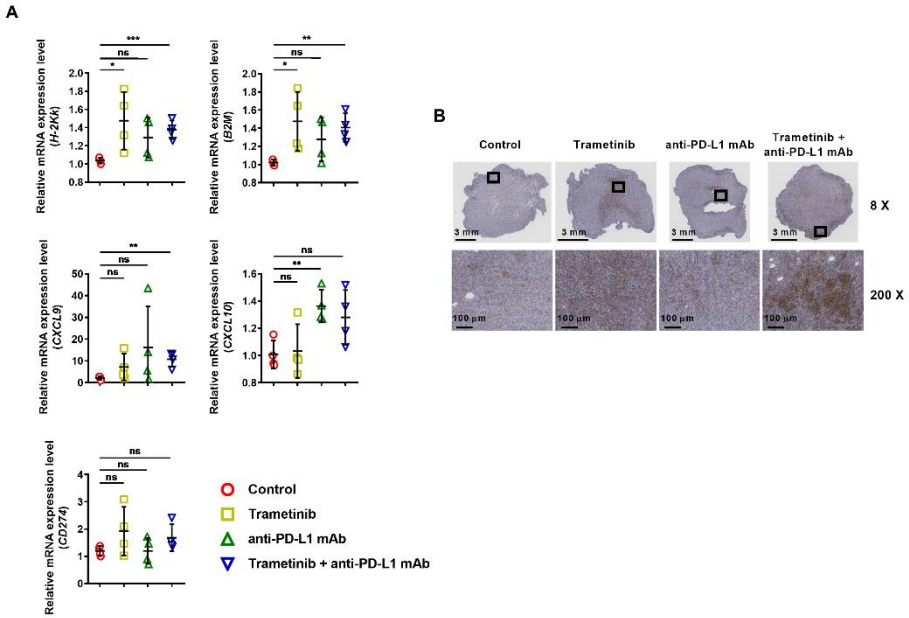

Figure 14. Confirmation of *in vitro* findings *in vivo* five days after treatment. A, Transcript levels of immune-related molecules were measured by performing qRT-PCR (n=4). **B,** Representative IHC images show PD-L1 expression within tumor tissue (n=3). Rectangles (top) indicate the enlarged areas (bottom).

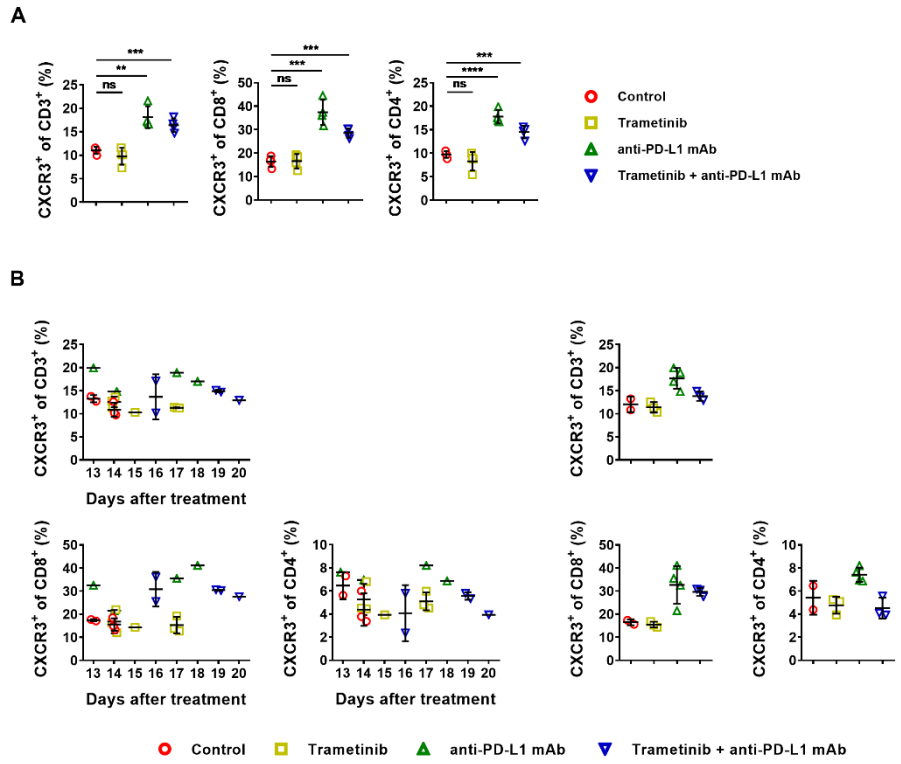

Figure 15. An anti-PD-L1 mAb enhances CXCR3 expression in splenic T cells. CXCR3 expression in splenic T cells was analyzed using flow cytometry after five days of treatment **(A)** (n=4) and at the endpoint **(B)** (n=4-7; sequential administration of drugs as in Fig. 17). **B,** Graphs represent CXCR3 expression from individual mice over time (left) and patterns of each group (right).

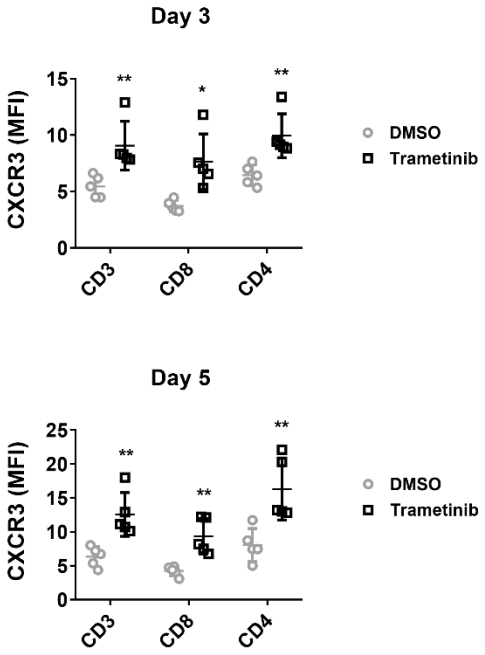

Figure 16. Trametinib upregulates CXCR3 expression in naive T cell subset derived from UCBMC. CXCR3 expression in naive T cells was analyzed using flow cytometry after three (top) and five days (bottom) of treatment with trametinib. The MFI levels were averaged from five different healthy donors, respectively. Error bars indicate SD.

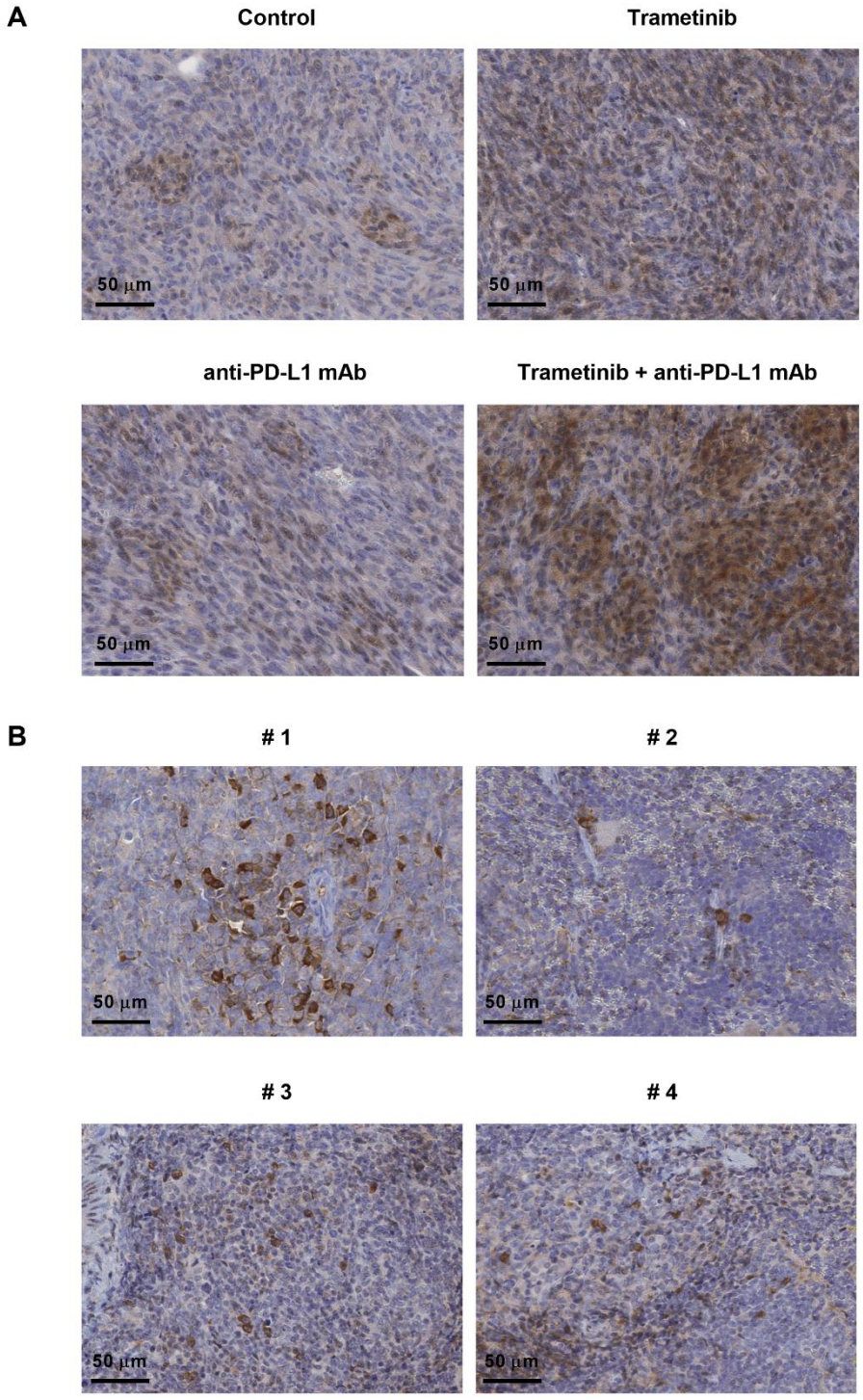
A
Control
Trametinib
50 μm
50 μm
anti-PD-L1 mAb
Trametinib + anti-PD-L1 mAb
50 μm
50 μm
B
1
2
50 μm
50 μm
3
4
50 μm
50 μm

Figure 17. Results of PD-L1 immunohistochemistry at 400 X magnification. A, Higher magnification of PD-L1 IHC shown in Fig. 13B. **B,** Staining results of relevant controls. Spleens from naïve (top) and tumor-bearing (bottom) mice were stained with anti-mouse PD-L1 mAb (n=2, respectively). Scale bar indicates 50 µm.

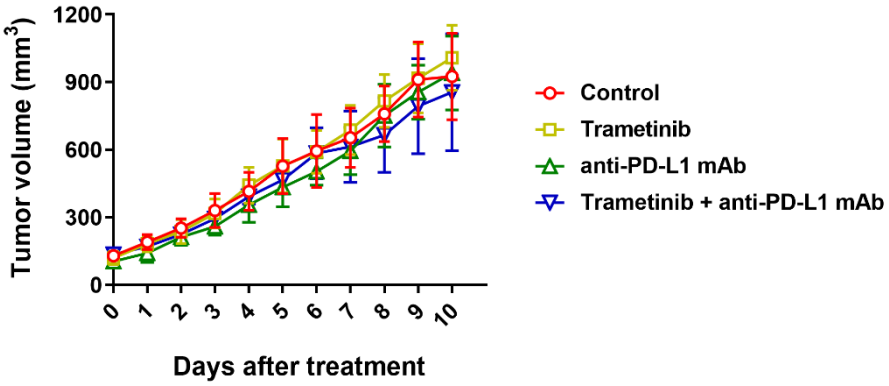

Figure 18. Same experiment as in Fig. 8B using BALB/c nude mice. A, Tumor-bearing BALB/c nude mice (n=5) were treated with trametinib (1 mg/kg) by oral gavage once daily and/or anti-PD-L1 mAb (10 mg/kg) by intraperitoneal injection twice weekly. Control mice received vehicle or isotype control.

Sequential treatment of trametinib and an anti-PD-L1 mAb inhibited tumor growth in a manner similar to the concurrent administration

Finally, we changed the treatment schedule from concurrent administration to sequential treatment to evaluate the immunomodulating effect of trametinib followed by an anti-PD-L1 mAb therapy. Trametinib treatment was given when the tumor grew to be palpable (at day -5), and an anti-PD-L1 mAb was administered five days later (day 0). However, we found that sequential treatment did not improve the effect on tumor growth, compared with concurrent administration (Fig. 19A). Moreover, similar to the previous experiments, trametinib or anti-PD-L1 mAb alone had no benefits in tumor control, and delayed tumor growth was seen only when they were combined. Again, overall immunological changes following combined therapy, including increased $CD8^+$ T cell infiltration in the tumor, were the same from endpoint analysis (Fig. 19B). It was demonstrated that, in this murine squamous cell carcinoma model, combining trametinib and an anti-PD-L1 mAb is a more potent intervention than either treatment alone, regardless of treatment sequence, although no remission was observed.

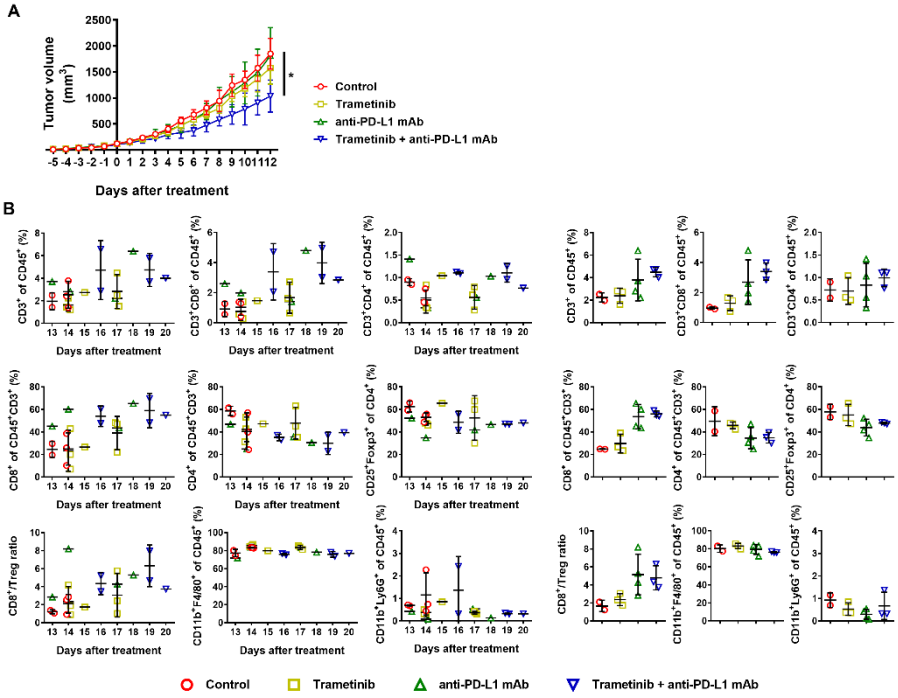

Figure 19. Sequential administration of trametinib and an anti-PD-L1 mAb inhibited tumor growth and increased T cell infiltration in a similar pattern as the concurrent administration. A, Tumor-bearing C3H mice (n=5-7) were given trametinib (day -5) and then an anti-PD-L1 mAb five days later (day 0). **B,** Cells were isolated from tumor tissues (n=4-7) for measuring of each immune cell subset at the endpoints. Graphs represent each immune cell subset from individual mice over time (left) and patterns of each group (right).

DISCUSSION

In this study, we found that treatment with the MEK inhibitor trametinib increases the expression of IFN-γ-induced immune molecules, including MHC class I, PD-L1, CXCL9 and CXCL10, which are associated with anti-tumor immunity. Inefficient tumor antigen presentation and recognition, through the loss or downregulation of MHC class I molecules on tumor cells is a well-known immune evasion mechanism. Although recent advances in anti-PD-1/PD-L1 blocking immunotherapies have shown remarkable clinical benefit, there are many non-responders as well as relapsed patients associated with downregulated MHC class I expression (36, 37). When tumors harbor alterations involved in antigen processing and presentation, several strategies can be explored to restore their expression (38, 39), including epigenetic modulation, IFN-γ pathway activation and inhibition of oncogenic signaling. In HNSCC, expression of MHC class I and β2m is also downregulated mostly in a reversible manner (40). Here, we demonstrated that the MEK inhibitor trametinib increases MHC class I expression at a concentration with moderate cellular cytotoxicity in human HNSCC cell lines. Simultaneous upregulation of PD-L1 expression by trametinib, with or without IFN-γ, was also observed in most cell lines tested.

MHC class I and PD-L1 are well-known downstream targets of IFN-γ signaling through the STAT1 pathway (31). PD-L1 expression is also regulated by various signaling pathways, including PI3K/Akt, MAPK, STAT3 and NF-κB pathways, both intrinsically (congeneric) and extrinsically (interaction with stromal cells) (41). Trametinib treatment acts through both the STAT1 and STAT3 pathways regulating MHC class I and PD-L1 expression. To this end, we found that trametinib-induced STAT3 activation upregulated MHC class I and PD-L1 in the SNU-1041 cell line. It is noteworthy that STAT3 is involved in the upregulation of MHC class I expression, because many signals involved

in immune suppression and tumor promotion are associated with STAT3 activation (42, 43). STAT3 is classically known to play an opposing role to STAT1- and NF-κB-mediated T helper type 1 immune responses, which are major transcriptional activators of MHC class I (44). However, these pathways are mechanistically interconnected with each other in a highly context-dependent manner. As an example, NF-κB pathway is responsible for both inflammation-induced tumorigenesis and anti-tumor immune response by regulating the expression of multiple inflammatory mediators and also could be activated by STAT3 signaling (45). Although the present study was able to obtain only implication for the relevance of STAT3 pathway in these phenomena, the underlying mechanism needs to be further deeply investigated for each cell line.

Based on the presence of effectors ($CD8^+$ T cells) and suppressors ($PD\text{-}L1^+$ cells), tumor microenvironments can be classified into four categories (46, 47). Using this classification system, type II ($TIL^-PD\text{-}L1^-$) and III ($TIL^-PD\text{-}L1^+$) tumors are predicted to respond poorly to anti-PD-1/PD-L1 mAb therapy. Therefore, it is important to attract $CD8^+$ T cells to tumors, as this may increase the therapeutic efficacy of immune checkpoint blockade therapies such as anti-PD-1/PD-L1 mAbs. Here, we observed that trametinib increases the expression of T cell recruitment chemokines (CXCL9 and CXCL10) in all human HNSCC cell lines examined, which may be further substantiated in the presence of T-cell derived IFN-γ.

We inferred that $CD8^+$ T cells mediate the functions of drugs by estimating the changes in total tumor-infiltrating $CD8^+$ T cells irrespective of antigen specificity because the mouse SCCVII tumor model lacks known TAAs. Despite a paucity of the specific TAA, the observed correlations between delayed tumor growth and the indicative of T cell activation, CD25, and IFN-γ production from *ex vivo* isolated T cells suggest that increased $CD8^+$ T cell

infiltration might contribute to suppress tumor progression. However, another issue is that there could be treatment-related toxicities because we do not currently know where the $CD8^+$ T cell response is directed. Although we did not observe toxicity defined by weight loss, appearance, behavior and mortality in any group of treatments in this study, severe side effects are occasionally observed in patients in clinic (data not shown), reflecting more detailed mechanisms of the drug action should be further investigated.

In addition, this was not the first study to evaluate the efficacy of a combining a MAPK pathway inhibitor and an anti-PD-1/PD-L1 mAb to enhance anti-tumor immune responses. However, our study is still meaningful in that most previous reports have examined this combination in MAPK mutant systems (19, 20, 48). Moreover, combination therapies using a MEK inhibitor and an anti-PD-1/PD-L1 mAb that are being examined in active clinical trials are primarily being performed in patients with *BRAF* mutant melanoma and *KRAS* mutant lung and colorectal cancer (NCT01988896). Recently, unlike expectations from phase Ib clinical trial, which shows encouraging tolerability and clinical activity in patients with colorectal cancer, expanding phase III trial, IMblaze370, did not meet its primary endpoint (NCT02788279). Several possible explanations for this failure might include: i) other co-stimulatory/-inhibitory molecules should be co-targeted to reach maximum T-cell activity (49, 50), ii) suppressive immune subsets like TAMs could mediate resistance to treatments (51-53). In current study, macrophages constituted substantial proportion in tumor tissues and the role of this subset as well as of other suppressive cells like Tregs need to be assessed to improve the drug efficacy. iii) Lastly, there could be a immunoregulatory role of the patient's microbiota, recently being proven to influence the anti-PD-1/PD-L1 mAb efficacy (54).

Based on our results, we propose that the combination of a MEK inhibitor and an anti-PD-1/PD-L1 mAb would be therapeutically beneficial for HNSCC

patients without MEK pathway mutations. Since immunotherapy still holds much promise, it is important to understand precise mechanisms behind the resistance to these therapies in future. In addition, further immunological studies using other small molecule inhibitors, especially those that target non-oncogene addiction, are required.

REFERENCE

1. Ferris RL. Immunology and Immunotherapy of Head and Neck Cancer. J Clin Oncol. 2015;33(29):3293-304.

2. Economopoulou P, Agelaki S, Perisanidis C, Giotakis EI, Psyrri A. The promise of immunotherapy in head and neck squamous cell carcinoma. Ann Oncol. 2016;27(9):1675-85.

3. Duray A, Demoulin S, Hubert P, Delvenne P, Saussez S. Immune suppression in head and neck cancers: a review. Clin Dev Immunol. 2010;2010:701657.

4. Chow LQ, Haddad R, Gupta S, Mahipal A, Mehra R, Tahara M, et al. Antitumor Activity of Pembrolizumab in Biomarker-Unselected Patients With Recurrent and/or Metastatic Head and Neck Squamous Cell Carcinoma: Results From the Phase Ib KEYNOTE-012 Expansion Cohort. J Clin Oncol. 2016.

5. Ferris RL, Blumenschein G, Jr., Fayette J, Guigay J, Colevas AD, Licitra L, et al. Nivolumab for Recurrent Squamous-Cell Carcinoma of the Head and Neck. N Engl J Med. 2016;375(19):1856-67.

6. Gotwals P, Cameron S, Cipolletta D, Cremasco V, Crystal A, Hewes B, et al. Prospects for combining targeted and conventional cancer therapy with immunotherapy. Nat Rev Cancer. 2017;17(5):286-301.

7. Lee Y, Auh SL, Wang Y, Burnette B, Wang Y, Meng Y, et al. Therapeutic effects of ablative radiation on local tumor require CD8+ T cells: changing strategies for cancer treatment. Blood. 2009;114(3):589-95.

8. Lugade AA, Moran JP, Gerber SA, Rose RC, Frelinger JG, Lord EM. Local radiation therapy of B16 melanoma tumors increases the generation of tumor antigen-specific effector cells that traffic to the tumor. J Immunol. 2005;174(12):7516-23.

9. Martins I, Kepp O, Schlemmer F, Adjemian S, Tailler M, Shen S, et al. Restoration of the immunogenicity of cisplatin-induced cancer cell death by endoplasmic reticulum stress. Oncogene. 2011;30(10):1147-58.

10. Mortara L, Orecchia P, Castellani P, Borsi L, Carnemolla B, Balza E. Schedule-dependent therapeutic efficacy of L19mTNF-alpha and melphalan combined with gemcitabine. Cancer Med. 2013;2(4):478-87.

11. Liu L, Mayes PA, Eastman S, Shi H, Yadavilli S, Zhang T, et al. The BRAF and MEK Inhibitors Dabrafenib and Trametinib: Effects on Immune Function and in Combination with Immunomodulatory Antibodies Targeting PD-1, PD-L1, and CTLA-4. Clin Cancer Res. 2015;21(7):1639-51.

12. Garrido G, Rabasa A, Sanchez B, Lopez MV, Blanco R, Lopez A, et al. Induction of immunogenic apoptosis by blockade of epidermal growth factor receptor activation with a specific antibody. J Immunol. 2011;187(10):4954-66.

13. Hughes PE, Caenepeel S, Wu LC. Targeted Therapy and Checkpoint Immunotherapy Combinations for the Treatment of Cancer. Trends Immunol. 2016;37(7):462-76.

14. Kang J, Demaria S, Formenti S. Current clinical trials testing the combination of immunotherapy with radiotherapy. J Immunother Cancer. 2016;4:51.

15. Morrissey KM, Yuraszeck TM, Li CC, Zhang Y, Kasichayanula S. Immunotherapy and Novel Combinations in Oncology: Current Landscape, Challenges, and Opportunities. Clin Transl Sci. 2016;9(2):89-104.

16. Boni A, Cogdill AP, Dang P, Udayakumar D, Njauw CN, Sloss CM, et al. Selective BRAFV600E inhibition enhances T-cell recognition of melanoma without affecting lymphocyte function. Cancer Res. 2010;70(13):5213-9.

17. Frederick DT, Piris A, Cogdill AP, Cooper ZA, Lezcano C, Ferrone CR, et al. BRAF inhibition is associated with enhanced melanoma antigen

expression and a more favorable tumor microenvironment in patients with metastatic melanoma. Clin Cancer Res. 2013;19(5):1225-31.

18. Liu C, Peng W, Xu C, Lou Y, Zhang M, Wargo JA, et al. BRAF inhibition increases tumor infiltration by T cells and enhances the antitumor activity of adoptive immunotherapy in mice. Clin Cancer Res. 2013;19(2):393-403.

19. Hu-Lieskovan S, Mok S, Homet Moreno B, Tsoi J, Robert L, Goedert L, et al. Improved antitumor activity of immunotherapy with BRAF and MEK inhibitors in BRAF(V600E) melanoma. Sci Transl Med. 2015;7(279):279ra41.

20. Ebert PJR, Cheung J, Yang Y, McNamara E, Hong R, Moskalenko M, et al. MAP Kinase Inhibition Promotes T Cell and Anti-tumor Activity in Combination with PD-L1 Checkpoint Blockade. Immunity. 2016;44(3):609-21.

21. Loi S, Dushyanthen S, Beavis PA, Salgado R, Denkert C, Savas P, et al. RAS/MAPK Activation Is Associated with Reduced Tumor-Infiltrating Lymphocytes in Triple-Negative Breast Cancer: Therapeutic Cooperation Between MEK and PD-1/PD-L1 Immune Checkpoint Inhibitors. Clin Cancer Res. 2016;22(6):1499-509.

22. Bendell JC, Kim TW, Goh BC, Wallin J, Oh DY, Han SW, et al. Clinical activity and safety of cobimetinib (cobi) and atezolizumab in colorectal cancer (CRC). Journal of Clinical Oncology. 2016;34(15).

23. Atefi M, Avramis E, Lassen A, Wong DJ, Robert L, Foulad D, et al. Effects of MAPK and PI3K pathways on PD-L1 expression in melanoma. Clin Cancer Res. 2014;20(13):3446-57.

24. Zhao Y, Adjei AA. The clinical development of MEK inhibitors. Nat Rev Clin Oncol. 2014;11(7):385-400.

25. Marur S, Forastiere AA. Head and neck cancer: changing epidemiology, diagnosis, and treatment. Mayo Clin Proc. 2008;83(4):489-501.

26. Molinolo AA, Amornphimoltham P, Squarize CH, Castilho RM, Patel V, Gutkind JS. Dysregulated molecular networks in head and neck carcinogenesis. Oral Oncol. 2009;45(4-5):324-34.

27. Angell TE, Lechner MG, Jang JK, LoPresti JS, Epstein AL. MHC class I loss is a frequent mechanism of immune escape in papillary thyroid cancer that is reversed by interferon and selumetinib treatment in vitro. Clin Cancer Res. 2014;20(23):6034-44.

28. Cardinali M, Pietraszkiewicz H, Ensley JF, Robbins KC. Tyrosine phosphorylation as a marker for aberrantly regulated growth-promoting pathways in cell lines derived from head and neck malignancies. Int J Cancer. 1995;61(1):98-103.

29. Hirst DG, Brown JM, Hazlehurst JL. Enhancement of CCNU cytotoxicity by misonidazole: possible therapeutic gain. Br J Cancer. 1982;46(1):109-16.

30. Hah JH, Zhao M, Pickering CR, Frederick MJ, Andrews GA, Jasser SA, et al. HRAS mutations and resistance to the epidermal growth factor receptor tyrosine kinase inhibitor erlotinib in head and neck squamous cell carcinoma cells. Head Neck. 2014;36(11):1547-54.

31. Meissl K, Macho-Maschler S, Muller M, Strobl B. The good and the bad faces of STAT1 in solid tumours. Cytokine. 2017;89:12-20.

32. Bu LL, Yu GT, Wu L, Mao L, Deng WW, Liu JF, et al. STAT3 Induces Immunosuppression by Upregulating PD-1/PD-L1 in HNSCC. J Dent Res. 2017;96(9):1027-34.

33. Wolfle SJ, Strebovsky J, Bartz H, Sahr A, Arnold C, Kaiser C, et al. PD-L1 expression on tolerogenic APCs is controlled by STAT-3. Eur J Immunol. 2011;41(2):413-24.

34. Marzec M, Zhang Q, Goradia A, Raghunath PN, Liu X, Paessler M, et al. Oncogenic kinase NPM/ALK induces through STAT3 expression of

immunosuppressive protein CD274 (PD-L1, B7-H1). Proc Natl Acad Sci U S A. 2008;105(52):20852-7.

35. Weng Y, Siciliano SJ, Waldburger KE, Sirotina-Meisher A, Staruch MJ, Daugherty BL, et al. Binding and functional properties of recombinant and endogenous CXCR3 chemokine receptors. J Biol Chem. 1998;273(29):18288-91.

36. Kim JM, Chen DS. Immune escape to PD-L1/PD-1 blockade: seven steps to success (or failure). Ann Oncol. 2016;27(8):1492-504.

37. Gettinger S, Choi J, Hastings K, Truini A, Datar I, Sowell R, et al. Impaired HLA Class I Antigen Processing and Presentation as a Mechanism of Acquired Resistance to Immune Checkpoint Inhibitors in Lung Cancer. Cancer Discov. 2017;7(12):1420-35.

38. Lampen MH, van Hall T. Strategies to counteract MHC-I defects in tumors. Curr Opin Immunol. 2011;23(2):293-8.

39. van der Burg SH, Arens R, Ossendorp F, van Hall T, Melief CJ. Vaccines for established cancer: overcoming the challenges posed by immune evasion. Nat Rev Cancer. 2016;16(4):219-33.

40. Cancer Genome Atlas N. Comprehensive genomic characterization of head and neck squamous cell carcinomas. Nature. 2015;517(7536):576-82.

41. Chen J, Jiang CC, Jin L, Zhang XD. Regulation of PD-L1: a novel role of pro-survival signalling in cancer. Ann Oncol. 2016;27(3):409-16.

42. Kortylewski M, Kujawski M, Wang T, Wei S, Zhang S, Pilon-Thomas S, et al. Inhibiting Stat3 signaling in the hematopoietic system elicits multicomponent antitumor immunity. Nat Med. 2005;11(12):1314-21.

43. Yu H, Kortylewski M, Pardoll D. Crosstalk between cancer and immune cells: role of STAT3 in the tumour microenvironment. Nat Rev Immunol. 2007;7(1):41-51.

44. Yu H, Pardoll D, Jove R. STATs in cancer inflammation and immunity: a leading role for STAT3. Nat Rev Cancer. 2009;9(11):798-809.

45. Lee H, Herrmann A, Deng JH, Kujawski M, Niu G, Li Z, et al. Persistently activated Stat3 maintains constitutive NF-kappaB activity in tumors. Cancer Cell. 2009;15(4):283-93.

46. Teng MW, Ngiow SF, Ribas A, Smyth MJ. Classifying Cancers Based on T-cell Infiltration and PD-L1. Cancer Res. 2015;75(11):2139-45.

47. Ock CY, Keam B, Kim S, Lee JS, Kim M, Kim TM, et al. Pan-Cancer Immunogenomic Perspective on the Tumor Microenvironment Based on PD-L1 and CD8 T-Cell Infiltration. Clin Cancer Res. 2016;22(9):2261-70.

48. Hu-Lieskovan S, Robert L, Homet Moreno B, Ribas A. Combining targeted therapy with immunotherapy in BRAF-mutant melanoma: promise and challenges. J Clin Oncol. 2014;32(21):2248-54.

49. Wang B, Zhang W, Jankovic V, Golubov J, Poon P, Oswald EM, et al. Combination cancer immunotherapy targeting PD-1 and GITR can rescue CD8(+) T cell dysfunction and maintain memory phenotype. Sci Immunol. 2018;3(29).

50. Wei SC, Duffy CR, Allison JP. Fundamental Mechanisms of Immune Checkpoint Blockade Therapy. Cancer Discov. 2018;8(9):1069-86.

51. Wang W, Marinis JM, Beal AM, Savadkar S, Wu Y, Khan M, et al. RIP1 Kinase Drives Macrophage-Mediated Adaptive Immune Tolerance in Pancreatic Cancer. Cancer Cell. 2018;34(5):757-74 e7.

52. Medler TR, Murugan D, Horton W, Kumar S, Cotechini T, Forsyth AM, et al. Complement C5a Fosters Squamous Carcinogenesis and Limits T Cell Response to Chemotherapy. Cancer Cell. 2018;34(4):561-78 e6.

53. Wang F, Zhang S, Vuckovic I, Jeon R, Lerman A, Folmes CD, et al. Glycolytic Stimulation Is Not a Requirement for M2 Macrophage Differentiation. Cell Metab. 2018;28(3):463-75 e4.

54. Oliva M, Spreafico A, Taberna M, Alemany L, Coburn B, Mesia R, et al. Immune Biomarkers of Response to Immune-Checkpoint Inhibitors in Head and Neck Squamous Cell Carcinoma. Ann Oncol. 2018.

국문초록

연구 목적: 현재 종양 면역 회피에 대한 이해의 진보는 두경부암을 포함한 암 치료에 있어서 면역 요법의 새로운 분야를 이끌어 내었다. 그러나 여전히 소수의 환자만이 항 PD-1/PD-L1 단일 클론 항체에 반응을 보인다. 본 연구에서는, 인간 두경부암 세포주에서 면역 관련 분자인 MHC class I, PD-L1 및 T 세포 유인 케모카인인 CXCL9 및 CXCL10 의 발현에 대한 MEK 억제제인 trametinib 의 효과를 조사했다. 그런 다음 우리는 두경부암을 위한 모델인 SCCVII 마우스 동종 종양 모델을 사용하여 생체 내에서 항 PD-L1 단일 클론 항체와 병용한 trametinib 의 치료 효능을 평가했다.

연구 방법: 6 개의 인간 두경부암 세포주 (SNU-1041, SNU-1066, SNU-1076, Detroit 562, FaDu 및 HN31) 및 마우스 편평 세포암 세포주 (SCCVII)를 사용하였다. 우리는 이 세포주를 사용하여 trametinib 처리 후 72 시간 뒤에 MTT 세포 생존율 분석을 수행했다. MHC class I 및 PD-L1 발현 수준은 trametinib 및 인터페론 감마를 처리한 후 유세포 계측법으로 분석하였다. PD-L1, Erk1/2, STAT1, STAT2, STAT3, STAT5 및 STAT6 의 발현은 웨스턴 블롯으로 분석하였다. STAT1, STAT3 및 STAT6 를 리포펙타민을 사용하는 siRNA 주입에 의해 유전자 발현 억제시켰다. Trametinib 처리 후 CXCL9 및 CXCL10 전사체의 발현 수준을 확인하기 위해 정량적 실시간 PCR 이 수행되었다. ELISA 및 유세포 분석법을 사용하여 CXCL9 및 CXCL10 의 단백질 수준을 결정하였다. 동종 마우스 SCCVII 편평 세포암 모델에서 MEK 억제제와 항 PD-L1 단일 클론 항체의 병용 치료 효과를 평가하였다.

연구 결과: Trametinib 에 의한 성장 억제는 적정한 감도 (6 개의 인간 세포 중 4 개에서의 IC_{50} 값이 10 nM 이상, 100 nM 이하)로 세포주 간에 가변적이었다. Detroit 562 와 FaDu 에서의 IC_{50} 값은 10 μM 이상이었다. Trametinib 은 인간 두경부암 세포주에서 MHC class I 과 PD-L1 발현을 상향 조절하였으며, 이는 STAT3 활성화를 통해 일어났다. 또한, trametinib 은 인간 두경부암 세포주에서 종양 조직으로의 T 세포 침윤과 연관되고, 인터페론 감마에 의해 증가하는 CXCL9 과 CXCL10 의 발현을 상향 조절했다. 마지막으로, 우리는 두경부암을 위한 SCCVII 동종 종양 모델을 사용하여 생체 내에서 항 PD-L1 단일 클론 항체와 조합된 trametinib 의 치료 효능을 평가하였다. PD-L1 차단이나 trametinib 치료는 각각 단독으로는 종양 성장에 영향을 미치지 않았지만, 병용 치료 시에 종양 성장을 유의하게 지연시켰다. 우리의 결과는 이 병용 치료에서 trametinib 이 종양 부위로의 $CD8^+$ T 세포 침윤을 증가시키고 항원 제시를 증가시키는 것을 보여주었으며, 이는 PD-L1 차단 효능의 증강과 연관될 수 있음을 보여주었다.

결론: 우리의 결과는 두경부암에서의 면역 회피 기전이 MEK 억제제와 항 PD-1/PD-L1 단일 클론 항체의 병용 요법에 의해 상쇄됨으로써 종양 성장이 저해될 수 있음을 시사한다.

.....

주요어 : 두경부암, MEK 억제제, 항 PD-1/PD-L1 단일 클론 항체, 면역적 인지, 면역 침윤

학 번 : 2015 - 30612